



Riverscale distribution of zooplankton in the St. Lawrence River in relation to hydrological networks, hydroperiods and local environmental gradients

Zofia E. Taranu · Pierre Legendre · Edith Cusson ·
Bernadette Pinel-Alloul 

Received: 15 October 2022 / Revised: 2 May 2023 / Accepted: 6 May 2023
© The Author(s), under exclusive licence to Springer Nature Switzerland AG 2023

Abstract We studied the community structure of crustacean zooplankton along the biogeographical zones of the St. Lawrence River (Québec, Canada), to evaluate how the riverscale hydrological network formed by water masses, and local-scale aquatic environment, influenced the distribution of crustacean groups (cladocerans, calanoids, cyclopoids and

harpacticoids) during the spring (high discharge) and summer (low discharge) hydroperiods. Zooplankton and environmental data were sampled at 52 sites forming 16 transects along the fluvial section zone (FSZ), the fluvial estuary zone (FEZ) and the estuarine transition zone (ETZ) of the St. Lawrence River in May and August 2006. We compared zooplankton community composition among biogeographical zones and fluvial lakes and across the fluvial estuarine continuum. Analyses were carried out using asymmetric eigenvector maps (AEM), redundancy analysis (RDA), and variation partitioning. Spatial distribution patterns revealed a complex river model. Riverscale discontinuities between the fluvial and estuarine transition zones, and the hydrological network of water masses in the fluvial zones, explained better the spatial zooplankton distribution patterns along the fluvial estuarine continuum than the local environment. Spatial variation in the flow network and environmental conditions were the main drivers of zooplankton distributions in spring whereas the flow network of water masses was the most influential factor in summer.

Handling editor: Gideon Gal

Guest editor: Koen Martens / A Homage to Henri J.F. Dumont, a Life in Science!

Supplementary Information The online version contains supplementary material available at <https://doi.org/10.1007/s10750-023-05259-7>.

Z. E. Taranu
Aquatic Contaminants Research Division, Environment and Climate Change Canada, ECCC, 105 McGill, 7th Floor, Montréal, QC H2Y 2E7, Canada
e-mail: zofia.taranu@ec.gc.ca

Z. E. Taranu · P. Legendre · E. Cusson ·
B. Pinel-Alloul (✉)
Département de Sciences Biologiques, Groupe de Recherche Interuniversitaire en Limnologie Et en Environnement Aquatique, GRIL-UdeM, Université de Montréal, Complexe Des Sciences, C. P. 6128, Succ. Centre-Ville, Montréal, QC H3C 3J7, Canada
e-mail: bernadette.pinel-alloul@umontreal.ca

P. Legendre
e-mail: pierre.legendre@umontreal.ca

E. Cusson
e-mail: edithcusson@hotmail.com

Keyword Asymmetric Eigenvector Maps (AEM) · Directional hydrological network and water quality · Ecological modelling · St. Lawrence River · Variation partitioning · Zooplankton spatial distribution patterns

Introduction

Riverine macrosystems comprise a hydrological network of connected and interacting riverine and upland habitats (McCluney et al., 2014). Large rivers are thus not only organized as a continuous longitudinal gradient, but generally composed of different water masses, including fluvial lakes or reservoirs, that cause discontinuities between upstream processes and downstream ecosystem dynamics (Ward & Stanford, 1983). They may also include a mosaic of habitats along their transversal dimension (shores to channel) such as littoral beds of vegetation and tributary plumes. Consequently, Thorp et al. (2006) considered large rivers as an array of hydrogeomorphic patches consisting of different ecological zones and biological communities. The complex interplay between factors driving habitat heterogeneity (distinct water masses across the transverse axis) versus homogeneity (continuous flow along the longitudinal axis) is expected to have an important impact on the distribution of aquatic communities in rivers.

Recognition of the longitudinal and transversal dimensions of rivers stimulated interest to assess the spatial structure and function of river biota (Thorp et al., 2006). Over the past few decades, several conceptual models have been developed to describe the patterns of biotic communities in river macrosystems (Thorp et al., 2008; Doretto et al., 2020). However, microorganisms such as zooplankton have been less studied compared to other organisms inhabiting riverine habitats, even though they constitute the basis of the foodweb for higher trophic levels (Thorp & Casper, 2003; Lair, 2006). According to the River Continuum Concept (RCC: Vannote et al., 1980) and the Riverine Productivity Model (RPM: Thorp & Delong, 1994), zooplankton biomass generally increases from upstream to downstream along the longitudinal gradient. According to the Serial Discontinuity Model (SDM: Thorp et al., 1994; Stanford & Ward, 2001), discontinuities such as confluences, fluvial lakes and reservoirs, may disrupt the longitudinal gradient. Zooplankton biomass per unit river length may decrease where tributary flow is strong, or increase in fluvial lakes which have longer water retention times (Basu et al., 2000a), or due to water release from reservoirs (Le Coz et al., 2017). Added to this, the Flood Pulse Model (FPC: Junk et al., 1989; Tockner et al., 2000) suggests that zooplankton

distribution and dynamics in floodplain rivers are influenced by seasonal patterns in flooding and lateral water discharge that expand or contract the connectivity with littoral vegetated and slackwater habitats (Casper & Thorp, 2007; Burdis & Hoxmeier, 2011). Recently, Humphries et al. (2014) combined the continuum, productivity, and flood pulse models (i.e. RCC, RPM and FPC) into a new unifying concept, the River Wave Concept (RWC), where river flow along the longitudinal and transversal axes configures different ecosystem stages and types of productivity (autochthonous vs allochthonous). There is still a lack of knowledge, however, on how the spatial pattern of zooplankton distribution fits with these different models in small and large rivers, representing simple or complex hydrological networks (Doretto et al., 2020).

Previous studies conducted in small temperate rivers in southern Ontario and western Quebec showed that flow along the longitudinal gradient was the main process structuring zooplankton biomass, where water residence time had a stronger (positive) effect than algal resources and nutrients on zooplankton (Basu & Pick, 1996, 1997). At the other extreme, zooplankton abundance was found to sharply decrease in the high-flowing Niagara River (Rozon et al., 2016) and during high spring discharge in the Danube River (Baranyi et al., 2002). Overall, studies have shown diversified and complex patterns across rivers, where zooplankton distribution is influenced by both the effects of longitudinal (created by fluvial lakes and reservoirs) and transversal (due to littoral vegetated banks and tributary plumes) discontinuities (Thorp et al., 1994; Viroux, 1997, 1999; Akopian et al., 2002; Tackx et al., 2004; Picard & Lair, 2005; Wahl et al., 2008; Havel et al., 2009; Dickerson et al., 2010; Le Coz et al., 2017).

In Canada, most studies conducted in large river ecosystems have focused on estuaries and marine bays (Bay of Fundy: Aubé et al., 2005; Mackenzie River-Beaufort Sea: Walkusz et al., 2010; St. Lawrence Estuary: Winkler et al., 2003; Simons et al., 2006). Few studies have evaluated the effects of hydrological network and environmental heterogeneity on zooplankton communities across a fluvial to estuary continuum (Akopian et al., 2002; Tackx et al., 2004). A unique opportunity to examine this question presented itself in the St. Lawrence River, one of the largest rivers in the world, composed of a mosaic of

heterogeneous hydrogeomorphic zones with strong longitudinal and transversal connectivity. During the past twenty years, a few studies have investigated how riverscape longitudinal gradients affect spatial patterns in zooplankton biomass (Basu et al., 2000a), functional diversity (Massicotte et al., 2014), and copepod community composition (Pinel-Alloul et al., 2011) within this riverine macrosystem. At the local scale, studies have investigated the distribution pattern of zooplankton over a few sites and transects at the outlet of Lake Ontario (Mills et al., 1981; Casper & Thorp, 2007; Twiss et al., 2010) and in littoral macrophyte beds of the St. Lawrence River's fluvial lakes (Basu et al., 2000b; Bolduc et al., 2016, 2020).

Analysing how hydrological and environmental processes affect the zooplankton spatial distribution in the St. Lawrence River is a difficult endeavour because of its longitudinal heterogeneity in riverine habitats (fluvial lakes and corridors as well as transitional estuarine zones), which display their own particular physical and biological properties and whose interconnectivity varies depending on the seasonal hydroperiods (high discharge during spring vs low discharge during summer). Moreover, the deep and fast flowing navigation channel running through the centre of the river may strengthen the transversal disconnection between littoral habitats of the north and south shores and form distinct and unmixed water masses down to the Québec City region where fresh waters are finally mixed and homogenized with estuarine waters. In this study, we evaluated, for the first time, the coupling between zooplankton distribution and different models of hydrological flow and mixing networks along the whole freshwater-estuarine continuum of the St. Lawrence River, while also considering local environmental changes in water conditions. Furthermore, by sampling two hydroperiods in May and August 2006, our study is distinctively positioned to compare the high (spring) and low (summer) discharge periods and their impacts on habitat connectivity and zooplankton distribution.

Our first objective was to identify, for each hydroperiod, crustacean community types along the biogeographical zones of the St. Lawrence River (fluvial, fluvial estuarine and estuarine transition zones). Because geomorphology and salinity gradients are known to modulate ecological processes along the fluvial estuarine continuum of the St. Lawrence River (CSL-Centre Saint-Laurent, 1996), we expected to

detect major riverscale longitudinal changes in zooplankton composition among the biogeographical zones from the fluvial lakes and corridor to the estuarine zone. We also expected to observe small-scale variations due to transversal discontinuity among water masses and mixing with tributaries in the fluvial zones. More generally, we expected the effects of hydrological factors (water masses distribution and connectivity) and local environment (water conditions) to differ between the two hydroperiods.

Our second objective was to quantify the relative importance of directional hydrological network and non-directional environmental processes on the zooplankton spatial distribution patterns in the fluvial zones of the St. Lawrence system during the spring and summer hydroperiods. We hypothesized that zooplankton spatial distribution along the fluvial continuum would be more strongly related to the longitudinal directional distribution of water masses and their partial transversal mixing than to local environmental water conditions. We also hypothesized that the directional hydrological process would have a greater effect than environmental conditions during the spring hydroperiod (high discharge and currents), whereas the inverse would be true during the summer hydroperiod (low discharge and stronger transversal discontinuities). To test these ecological hypotheses, we created four different hydrological models (connection diagrams) for each hydroperiod, differing by the importance given to unidirectional flow, mixing of water masses and confluence with tributaries in the fluvial zones.

Materials and methods

St Lawrence River biogeographical zones and water masses

The St. Lawrence River (SLR) macrosystem, including the Great Lakes, is one of the largest freshwater systems in the world, draining a 1,344,200 km² watershed in Canada and the United States. The fluvial estuarine continuum covers three biogeographical zones (Fig. 1) (CSL-Centre Saint-Laurent, 1996). The fluvial section zone (FSZ) is 240 km long (from Cornwall (Ontario) to the Lake Saint-Pierre (Québec) outlet) and up to 10 km wide. This freshwater zone encompasses Lake Saint-François (LSF), Lake

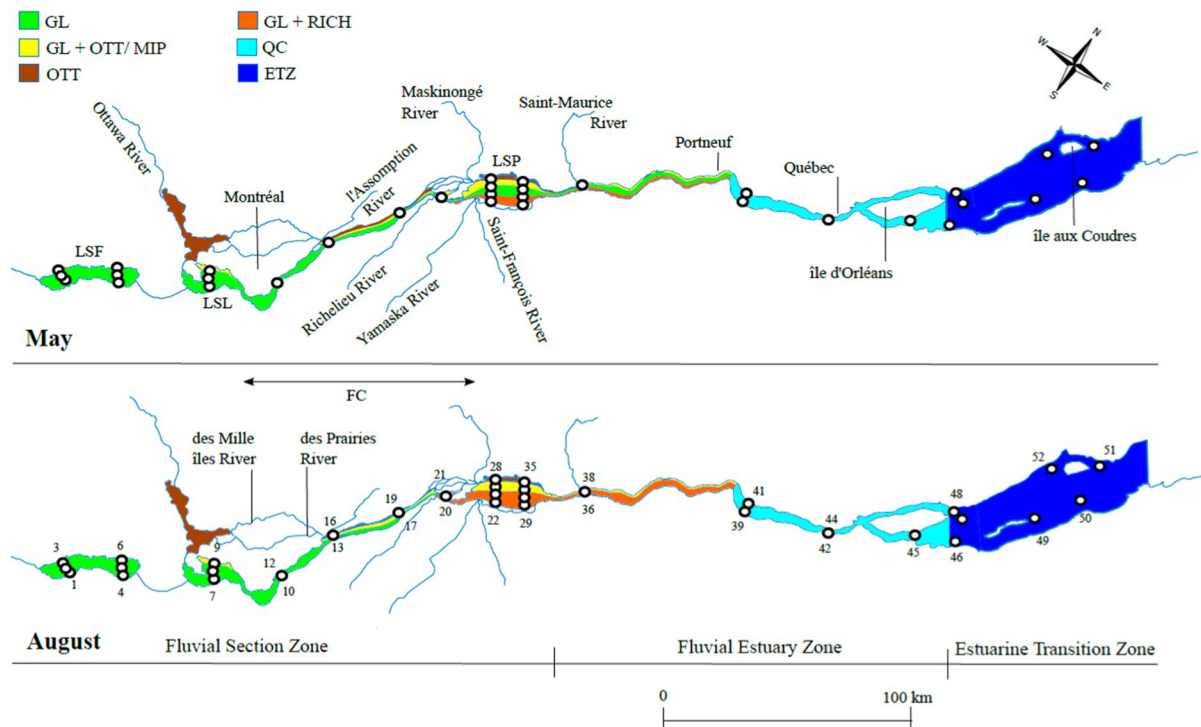


Fig. 1 Water masses of the St. Lawrence River (SLR) in **a** May and **b** August 2006. Green=Great Lakes water (GL), yellow=mix of GL, Ottawa River (OTT) and Milles Îles and des Prairies Rivers (MIP), brown=mix of OTT with Assomption (ASS) and Maskinongé (MASK) Rivers, orange = mix of

GL and Richelieu River (RICH), blue=Québec City waters (QC). FSZ=fluvial section zone, FEZ=fluvial estuarine zone, ETZ=estuarine transition zone. 56 sampling sites were distributed across 16 transects in the SLR

Saint-Louis (LSL), the fluvial corridor (FC) downstream of Montréal and Lake Saint-Pierre (LSP). The fluvial lakes are wide, slow flowing ($<0.3 \text{ m}\cdot\text{s}^{-1}$ except in the central navigation channel) and shallow, with depth averaging 6 m in LSF and 3 m in LSL and LSP, whereas the fast flowing ($1 \text{ m}\cdot\text{s}^{-1}$) navigation channel is 11.3 to 15 m deep. They are extensively colonized by submerged macrophyte beds (Hudon, 1997; Basu et al., 2000b) which create slow-flowing littoral areas isolated from the rapidly circulating central channel. This transversal discontinuity limits the exchanges between the north, south and central water masses. The fluvial estuarine zone (FEZ) stretches more than 160 km from the LSP outlet to the eastern tip of Île d'Orléans. River width ranges from 870 m near Québec City to 15 km at the eastern end of Île d'Orléans. Average water depth in the main channel varies from 13 to 40 m. The FEZ is composed of fresh waters but shows significant semidiurnal tides (averaging 4.1 m) at Québec City. Finally, the

estuarine transition zone (ETZ) in the upper estuary covers about 100 km from Île d'Orléans up to Île aux Coudres, with an average width of 17 km and depth varying from 100 to 300 m. In this zone, high-intensity flow and strong tides cause fresh and salt water mixing, strong upwelling currents and significant sediment resuspension.

The hydrology of the river segment considered in this study is complex. The hydrological network of the SLR is composed of six water masses with different physical and chemical characteristics, flowing side by side in the fluvial lakes and corridor, mixing slightly or not at all for long distances, and differently during spring and summer (Fig. 1). The spatial distribution patterns of water masses during the two sampling expeditions were established using the 2D convection–diffusion DISPERSIM model (Champoux & Morin, 2007) and the hydrodynamic HYDROSIM model (based on discharge, water level and conductivity; CSL-Centre Saint-Laurent, 1996). In May,

in the FSZ, clear waters originating from the Great Lakes (GL: green on the map) fed the LSF and most of LSL and the main channel in the FC and FEZ. The coloured and humic waters from the Ottawa River (OTT: brown) filled Rivers Mille Îles and Des Prairies (MIP) north of Montréal and flowed in the northern portion of the fluvial corridor (FC). Along the north shore of LSL and LSP, the OTT waters mixed with the GL waters (GL+OTT/MIP: yellow) while receiving brown waters of tributary inputs from Rivers Assomption (ASS) and Maskinongé (MASK) (brown). In the south shore of LSP, the mixing of the Richelieu River and the GL formed another main water mass (GL+RICH: orange) including tributary inputs of the Yamaska and Saint-François Rivers that flowed down to Québec. In August, the transversal discontinuity was more pronounced as OTT and GL mixed waters (GL+OTT/MIP: yellow) occupied almost the whole northern portion of LSL, FC and LSP. In the southern portion of the river, the GL water mass flowing from LSF was replaced by the Great Lakes and Richelieu River mixed waters (GL+RICH: orange) in LSP and downstream. During both hydroperiods, water masses coming from LSP flowed in a laminar way before they reached Québec City. There, waters were homogenized, forming the Québec City waters (QC: light blue) up to Île d'Orléans. Then, flowing east, they met the estuarine transition waters (ETZ: dark blue) near the eastern tip of Île d'Orléans.

Sampling and analysis of environmental and zooplankton variables

Zooplankton and environmental data were collected during two cruises aboard the *Lampsilis* research vessel in the spring (May 23rd to 30th) and summer (August 8th to 15th) of 2006. A total of 52 sites, distributed along 16 transversal transects, were visited in the three biogeographical zones (Fig. 1, white circles). Transects were positioned perpendicularly to the main east-to-west axis of the SLR. In the fluvial section (FSZ), a total of 35 sites were sampled; they were distributed along 9 transects in LSF (sites 1–6), LSL (sites 7–12), FC (sites 13–21), and LSP (sites 22–35). In the fluvial estuarine zone (FEZ), a total of 10 sites were distributed along 3 transects (sites 36–44) and one site (45) south of Île d'Orléans. In the estuarine transition zone (ETZ), 3 sites were sampled

along a transect at the eastern tip of Île d'Orléans (sites 46–48) and 4 sites on the north and south shores (sites 49–52). Meteorological conditions were uniform during each sampling cruise; water mass stability was validated by examining satellite images.

We measured several variables at each site to assess local environmental heterogeneity in water conditions (Table 1). Water temperature (°C), conductivity (Cond.), turbidity (NTU), pH and dissolved oxygen (DO) were measured in situ using a Conductivity Temperature Depth profiler (CTD: YSI 6600 EDS-M sensor array, Yellow Spring Instruments). We determined underwater profiles of light irradiance (PAR: 350–800 nm) using a spectroradiometer-fluorometer (HFT: Satlantic hyperpro-Wetlab C Star). Water samples were collected at each site using an 8 L GO-Flow water sampler (Model 1080; General Oceanics) at ~1 m below surface. To measure chlorophyll *a* (Chl *a*), dissolved organic carbon (DOC), total nitrogen (TN), total phosphorus (TP), total dissolved solids (TDS) and chromophoric dissolved organic matter (aCDOM), water subsamples were drawn from GO-Flow bottles into acid-washed polyethylene bottles. Chl *a* concentrations were measured with a Turner Designs 10–005R fluorometer, after sonication and 24-h extraction in 90% acetone at 4°C in the dark (Parsons et al., 1984). For TN and TP analyses, samples were prefiltered on 45 mm diameter, 0.7-µm pore size GFF filters (Millipore) and kept frozen until analysis performed according to A.P.H.A (1998). DOC concentrations were determined with a total organic carbon analyzer (TOC-1010; OI Analytical, College Station, Texas, USA) by sodium persulfate digestion. CDOM absorbance (aCDOM) was measured with a Shimadzu UV-2401PC UV-Vis spectrophotometer (Shimadzu, Columbia, Maryland, USA) according to Frenette et al. (2006) and Massicotte & Frenette (2011).

Crustacean zooplankton was sampled at each site using a conical net (1 m mouth opening, 153 µm mesh size) hauled horizontally at 1-m depth. Net filtered volume was measured with a flowmeter (General Oceanic). Upon collection, samples were split into fractions with a Folsom plankton sample splitter. One-eighth of each sample was reserved for taxonomy and transferred into a 250 ml plastic bottle. Zooplankton was narcotized with carbonated water and preserved in a buffered 4% sugar-formaldehyde solution (Prepas, 1978). In the laboratory, subsamples

Table 1 Water characteristics in the three biogeographical zones of the St. Lawrence River during the spring (May) and summer (August) 2006 hydroperiods

May 2006	FSZ		FEZ		ETZ	
	Mean \pm SD	Range	Mean \pm SD	Range	Mean \pm SD	Range
Temperature ($^{\circ}$ C)	12.8 \pm 0.7	11.6–14.2	13.3 \pm 0.3	12.8–13.8	12.3 \pm 1.9	7.7–13.8
pH	7.9 \pm 0.2	7.5–8.1	7.8 \pm 0.1	7.6–7.9	7.8 \pm 0.1	7.7–7.8
Dissolved oxygen (DO mg.L ⁻¹)*	10.2 \pm 0.3	9.6–10.8	10.0 \pm 0.2	9.6–10.2	10.1 \pm 0.2	9.9–10.3
Conductivity (Cond. μ S.cm ⁻¹)	189.4 \pm 43.1	99.0–232.0	160.4 \pm 49.4	23.5–192.4	3695 \pm 6339	176.6–18,710
Total dissolved solids (TDS mg.L ⁻¹)	94.0 \pm 21.9	49.0–119.0	78.6 \pm 24.0	12.0–91.0	653.7 \pm 761.1	85.0–1705
Turbidity (NTU)	7.3 \pm 5.4	0–18.7	10.3 \pm 2.2	6.6–14.2	47.5 \pm 35.6	10.3–101.2
Chlorophyll <i>a</i> (Chl <i>a</i> μ g.L ⁻¹)	3.0 \pm 0.7	1.4–4.3	3.4 \pm 0.7	2.8–4.9	5.5 \pm 5.3	0.9–22.3
Total nitrogen (TN mg.L ⁻¹)	3.4 \pm 0.6	2.2–4.5	2.5 \pm 1	1.1–4.2	2.8 \pm 1.2	1.0–5.2
Total phosphorus (TP μ g.L ⁻¹)	36.4 \pm 19.2	8.4–83.7	51.7 \pm 16.8	20.4–72.6	157.7 \pm 141.6	28.4–475.3
Dissolved organic carbon (DOC mg.L ⁻¹)	4.6 \pm 1.6	2.4–9.6	5.7 \pm 1.7	4.1–9.6	7.2 \pm 9.8	3.0–39.6
PAR light extinction coefficient (PAR m ⁻¹)	1.8 \pm 0.8	0.5–3.3	2.3 \pm 0.3	1.9–2.7	4.6 \pm 2.5	1.5–10.2
Chromophoric DOM absorption (aCDOM m ⁻¹)	8.1 \pm 5.5	1.6–24.2	12.1 \pm 3.5	8.9–21.0	7.8 \pm 2.6	4.7–11.3
August 2006	FSZ		FEZ		ETZ	
	Mean \pm SD	Range	Mean \pm SD	Range	Mean \pm SD	Range
Temperature ($^{\circ}$ C)	23.4 \pm 0.8	20.3–24.6	22.5 \pm 0.6	21.1–23.2	20.5 \pm 3.5	12.2–23.2
pH	8.3 \pm 0.3	7.7–8.8	8.2 \pm 0.2	7.7–8.4	7.9 \pm 0.2	7.7–8.3
Dissolved oxygen (DO mg.L ⁻¹)*	–	–	–	–	–	–
Conductivity (Cond μ S.cm ⁻¹)	241 \pm 53	91–298	206 \pm 61	37–248	5242 \pm 8173	218–23 700
Total dissolved solids (TDS mg.L ⁻¹)	100.2 \pm 21.4	36.0–119.0	87.3 \pm 25.9	16.0–106.0	771.8 \pm 754.9	93.0–1705
Turbidity (NTU)	7.8 \pm 18.2	0.0–98.2	7.7 \pm 2.8	2.5–12.5	44.0 \pm 42.1	1.8–120.1
Chlorophyll <i>a</i> (Chl <i>a</i> μ g.L ⁻¹)	2.7 \pm 1.6	0.9–7.0	2.9 \pm 1.2	1.8–6.0	9.7 \pm 13.4	0.6–54.8
Total nitrogen (TN mg.L ⁻¹)	2.7 \pm 1.1	0.5–5.2	2.6 \pm 0.7	1.5–3.7	2.3 \pm 0.9	0.9–3.6
Total phosphorus (TP μ g.L ⁻¹)	15.3 \pm 8.9	4.5–44.7	19.8 \pm 5.0	12.2–28.5	62.6 \pm 49.4	17.5–150.6
Dissolved organic carbon (DOC mg.L ⁻¹)	3.7 \pm 1.8	2.1–10.5	4.3 \pm 1.2	3.3–7.4	3.7 \pm 0.8	2.0–5.4
PAR light extinction coefficient (PAR m ⁻¹)	1.6 \pm 1.0	0.4–4.9	1.9 \pm 0.3	1.7–2.6	4.5 \pm 3.8	0.9–14.5
Chromophoric DOM absorption (aCDOM m ⁻¹)	5.5 \pm 6.2	0.8–31.4	7.8 \pm 5.8	4.1–24.1	5.0 \pm 1.7	2.4–6.7

*Dissolved oxygen (DO) data were not available in August due to damage to the YSI sensor

were taken with a large-opening pipette, transferred to a Ward rotative cell and analysed under a stereomicroscope (Ward, 1995). Zooplankton organisms were sorted into different taxonomic groups (cladocerans, calanoid, cyclopoid and harpacticoid copepods) up to a total of 100 animals. Cladocerans and copepods were identified to species when possible or at least to the genus level. The copepodid stages (C1–C5) were categorized to appropriate suborders (Calanoida, Cyclopoida, Harpacticoida), whereas nauplii were not counted because the large net mesh size (153 μ m) cannot sample efficiently these small instars of copepods. Identification of cladocerans was based

on Edmonston (1959), Amoros (1984) and Hebert (1995). Identification of copepods followed Hudson et al. (2003), Lesko et al. (2003a, 2003b), Lacroix (1981), Balcer et al. (1984), Huys et al. (1996), Edmondson (1959) and Smith & Fernando (1978). Counts of crustacean species were expressed as numbers of individuals per cubic metre, accounting for subsampling fractionation during field collection and microscopic analysis. We determined zooplankton community typology within each hydroperiod by spatially constrained clustering (Guénard & Legendre, 2022) computed with the function `constr.hclust` of the `{adespatial}` package (Dray et al., 2022) in R

statistical computing (R Development Core Team, 2022).

Flow modelling and statistical analyses

For each hydroperiod, sampling sites were positioned in connection diagrams (flow models of water mass distributions) for the fluvial (FSZ) and fluvial estuarine (FEZ) zones (stations 1–44), with colour codes reflecting different water mass categories (Fig. 2). Unfortunately, several sampling sites were not sampled (4 and 6 in May; 10, 15, 16, 22, 28, 29 and 35 in August) due to a technical problem with the measurement equipment onboard. Sites 9 and 22 were not considered in May and August because their water mixes were incompatible with those of the other sampling sites of the network. For our analysis, we created six water mass categories for the Great Lakes waters (GL: green rectangle),

the mixed waters of the Great Lakes and the Ottawa River (GL+OTT: yellow ellipse in May) or the Mille Îles and des Prairies Rivers (GL+MIP: yellow ellipse in August), the mixed waters of the Ottawa and Assomption Rivers (OTT+ASS: brown rhomb in May), the mixed waters of the Ottawa and Maskinongé Rivers (OTT+MASK: grey stars in May), the mixed waters of the Great Lakes and the Richelieu River (GL+RICH: orange cross) and the Québec City waters (QC: blue hexagons) that were attributed to the sites. 2D convection–diffusion DISPERSIM and hydrodynamic HYDROSIM models were used to provide the percentages of these six original water masses within the water column at each site (see Table S1, supplemental material). Edges (links) relating two sites, or a tributary to a site, were established based on the modelled contribution of an upstream site to the water of its target site.

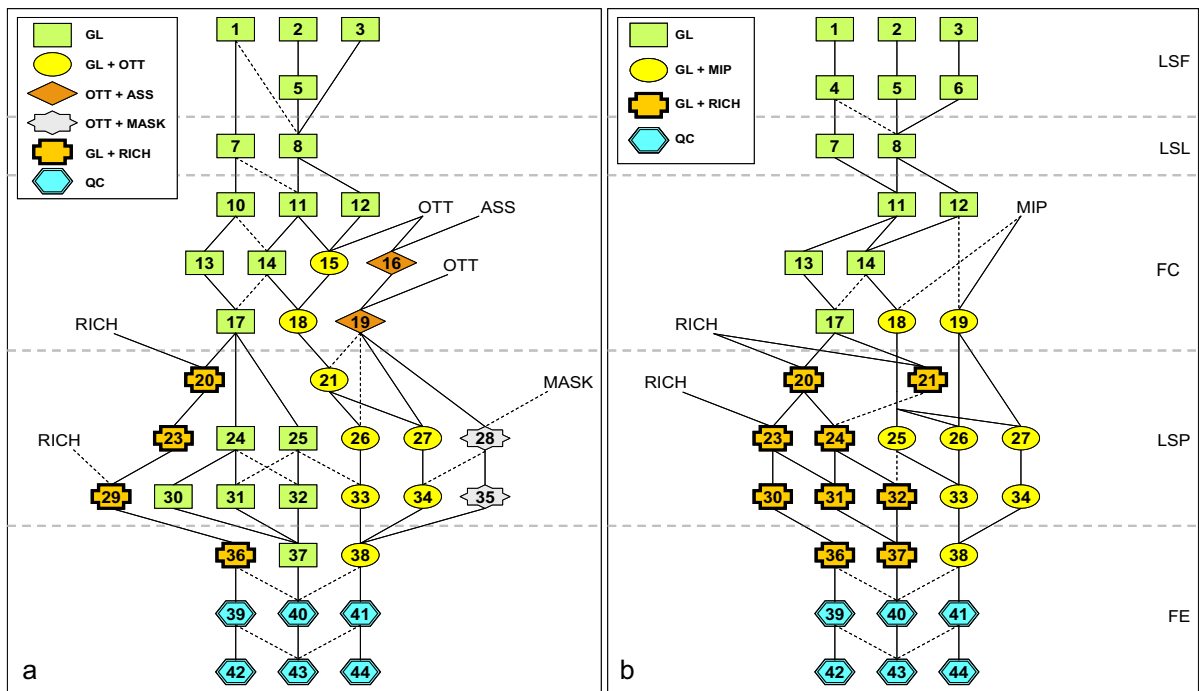


Fig. 2 Connection diagrams used **a** in May and **b** in August to generate the AEM eigenfunctions. The river flows from top to bottom of the maps. Each symbol is identified by a site number. The form and colour of a symbol relates a site to a water mass category: green rectangle=Great Lakes water (GL), yellow ellipse=mix of GL and Ottawa River (OTT) or Mille Îles and des Prairies Rivers (MIP), brown rhomb=mix of OTT and Assomption River (ASS), grey stars=mix of

OTT and Maskinongé River (MASK), orange cross=mix of GL and Richelieu River (RICH), blue hexagon=Québec City waters (QC). *LSF* Lake Saint-François, *LSL* Lake Saint-Louis, *FC* Fluvial Corridor, *LSP* Lake Saint-Pierre, *FE* Fluvial Estuary. Dotted lines represent weak edges (low weight). The fictitious site 0, the weights on the edges and their identification numbers are not shown to simplify the figure

Using the connection diagrams represented in Fig. 2 as the starting models, which contain the maximum number of edges, we then created, for each hydroperiod, four connection diagrams based on discharge and on physical–chemical data, and by consulting water mass maps (Centre Saint-Laurent—CSL, 1996). The four flow models differed by the importance given to the mixing of water masses and the influence of the tributaries. These models are as follows: ‘*Mixing with tributaries*’ (starting point shown in Fig. 2), ‘*Mixing without tributaries*’, ‘*No mixing with tributaries*’ and ‘*No mixing without tributaries*’. To obtain the four different models, we removed some edges in accordance with each specific model; for models ‘*without tributaries*’, we simply removed edges connecting tributaries to the network, for the ‘*no mixing*’ models, we removed edges considered weak (dotted lines in Fig. 2). The connection diagrams (site-by-edge matrices) and percentages of water masses (weight vector) were then used as inputs to the Asymmetric Eigenvector Maps (AEM) method to generate directional connection diagrams. AEM is an eigenfunction-based spatial filtering technique that was developed for situations where a directional process may influence a response variable along a gradient (Blanchet et al., 2008a, 2011; Legendre & Legendre, 2012; Borcard et al., 2018). The method can allow one to specify weights to edges to modulate the strength of the directional connections. We created and constructed the AEM variables used in this study following the calculation methods described by Blanchet et al. (2008a, 2011) (for details see Table S2, supplemental material); the AEM algorithm is also described through an example in Legendre & Legendre (2012, Sect. 14.3).

Briefly, for each hydroperiod, (1) site-by-edge matrices (Tables S2a, b, supplemental material) were written manually to represent the connection diagrams. To build these matrices, we first emphasized an upstream to downstream (top to bottom of Fig. 2) flow direction by adding a site 0 (‘Origin’, not shown) upstream of the study sites. The origin was connected to the most upstream study sites (sites 1, 2 and 3) as recommended by Blanchet et al. (2008a, 2011). Codes 1 were given to all edges (columns) that link a target site (row) to the origin (site 0) or stand along any downstream path between the target site and the origin. All edges that did not connect a target site to the origin received a code 0. (2) We then created

two options for each of the four connection diagrams either using weights, or not. For the model option without weights, all edges received equal weights. For the model options with weights on edges, edges were given weights by multiplying the values in each column of the site-by-edge matrix by the corresponding value in a weight vector (Tables S2c–d, supplemental material). To compute the weights on the edges, we used the initial water mass percentage data (Table S1, supplemental material), where each site received a mixture of water masses indicated in percentages. We evaluated the contribution of an upstream site to the connected sites downstream on the basis of those water mass percentages. Simple calculations were used to determine the percentage of one water mass at one site reaching a connected site downstream. For example, in May, site 18 (Table S1, supplemental material) was composed of 69% of Great Lakes (GL) water and of 31% of Ottawa River (OTT) water. Two upstream sites (site 14: 100% of GL: site 15: 50% of GL and 50% of OTT) were connected to site 18 (Fig. 2a). We assessed the proportion of the Ottawa River (OTT) water mass (site 15) reaching site 18 as follows: $31/50 * 100 = 62\%$. Thus, site 15 water contributed 62% of the water reaching site 18, and the remainder (38%) was considered to be water from site 14. In this way, for the starting point model (‘*Mixing with tributaries*’), the sum of the incoming edge weights into a site is always 100%. When we did not know the exact water mass composition (sites 1 to 8, 36 to 44), we distributed evenly the total weight (100%) among the incoming edges. For example, sites 39, 40 and 41 are all connected to site 43 (Fig. 2); thus, the three edges entering site 43 each had a weight of 33.3%. The edges with weights under 20%, as well as some other doubtful edges, were considered to be weak (dotted lines in Fig. 2) and were thus removed from the ‘*No mixing*’ models, as mentioned above. Finally, (3) to obtain the AEM variables, we performed a singular value decomposition (SVD) of the [weighted] site-by-edge matrices after centring them by columns. Steps 2 and 3 can be performed by the *aem()* function of the R-language package {adespatial} (Dray et al., 2022).

To determine the best AEM model for each hydroperiod, we computed a global redundancy analysis (RDA) for each set of AEM variables created from each of the four flow models (each with or without weights on edges), using as response matrix

the zooplankton data (crustacean groups) submitted to different transformations (Hellinger, chord, log-chord and chi-square) (Legendre & Gallagher, 2001; Legendre & Borcard, 2018). The flow model and transformation combinations that produced the best explanations (highest R^2_a) for each survey were identified. The AEM variables in the retained models were submitted to a forward selection procedure to choose a single best model for each hydroperiod, based on the resulting adjusted R-square (R^2_a) (Blanchet et al., 2008b). Bubble plots representing the significant RDA axes of zooplankton distribution modelled by the best flow model in May and August were drawn to display the zooplankton spatial patterns (see Fig. S1, supplemental material). A similar selection process was performed for dbMEMs (constructed using the *dbmem()* function from the {adespatial} package in R) and environmental data. dbMEM is a non-directional method of spatial analysis (Borcard & Legendre, 2002). Its algorithm is also described in Legendre & Legendre (2012, Sect. 14.1). After performing forward selection on AEMs, dbMEMs and environmental variables, we computed a variation partitioning (Borcard et al., 1992) of the zooplankton data between AEM (directional hydrological process), dbMEM (non-directional spatial structure) and environmental (local water conditions) variables. This was done using function *varpart()* from package {vegan} (Oksanen et al., 2022) in R statistical computing (R Development Core Team, 2022).

Results

Zooplankton community structure

In total, 67 crustacean species were identified, including 23 cladocerans, 8 calanoids, 17 cyclopoids and 19 harpacticoids (Table S3, supplemental material). Over the two hydroperiods (May and August), species richness was higher in the fluvial zones (FSZ: 44–55, FEZ: 29–35) than in the estuarine transition zone (ETZ: 12–19). Opposite to species richness, abundance of crustaceans during the two hydroperiods was relatively low in the FSZ (329–346 ind. m^{-3}) and the FEZ (291–429 ind. m^{-3}) but very high in the ETZ (1584–2946 ind. m^{-3}) (Table 2). Coarse community structure (group dominance) in the fluvial lakes (LSF, LSL, LSP) and corridors (FC, FEZ) differed greatly

between the two hydroperiods (Fig. 3). The cyclopoid copepods were dominant in May across all fluvial zones. In August, the cladocerans and the calanoids were generally dominant, although the relative abundance of the cyclopoids and harpacticoids was higher in FC and LSL. In the FEZ, cyclopoids were dominant in May and replaced by the calanoids in August. In the ETZ, zooplankton community was relatively stable and dominated by calanoids during the spring and summer hydroperiods.

Zooplankton species composition clearly differed at the scale of the river between the fluvial and estuarine transition zones, and also at smaller scale among the fluvial lakes and corridors, as well as between the spring and summer hydroperiods (Fig. 4; Table 2; see also Table S3 for details). In May, cladoceran species were dominated by *Bosmina* Baird, 1845 over all zones and *Chydorus* Leach, 1816 ranked second in all fluvial lakes (LSF, LSL, LSP) and corridor (FC), followed by *Daphnia* O. F. Müller, 1785 in LSF and FC (Fig. 4a). In August, *Bosmina* remained dominant except in LSF; however, other daphnids (*Daphnia*, *Ceriodaphnia* Dana, 1853) and chydorids (*Chydorus*, *Camptocercus* Baird, 1843, *Alona* Baird, 1850) increased in relative abundance in fluvial lakes (LSF, LSP) and corridors (FC, FEZ) (Fig. 4b). Calanoid copepods were clearly more abundant in the ETZ than in other fluvial zones and calanoid species composition differed greatly between spring and summer hydroperiods (Fig. 4c–d). In the ETZ, the marine calanoid species *Acartia longiremis* (Lilljeborg, 1853) was dominant in May and replaced by the epibenthic and euryhaline species *Eurytemora affinis* (Poppe, 1880) in August. The freshwater species (*Epischura lacustris* S. A. Forbes, 1882, *Leptodiatomus sicilis* (S. A. Forbes, 1882), *L. minutus* (Lilljeborg in Guerne and Richard, 1889) and *Skistodiatomus oregonensis* (Lilljeborg in Guerne and Richard, 1889)) were present in low abundance in May and replaced by *Eurytemora affinis* in August in all zones. Cyclopoid copepods showed clearly different compositions between hydroperiods (Fig. 4e–f). The freshwater pelagic species *Diacyclops thomasi* (S. A. Forbes, 1882) was dominant in May, whereas the brackish (*Halicyclops fosteri* M. S. Wilson, 1958) and epibenthic species (*Eucyclops pectinifer* Cragin, 1883, *E. prionophorus* Kiefer, 1931) were dominant in August. Harpacticoid copepods were

Table 2 Abundance (mean \pm SD; ind·m⁻³) of 4 major crustacean groups (and dominant taxa) in each biogeographical zone of the St. Lawrence River in May and August 2006

	Abundance		
	May		
	FSZ	FEZ	ETZ
	N=33	N=10	N=7
Cladocerans	82.0 \pm 94.6	72.2 \pm 52.4	23.9 \pm 33.9
<i>Bosmina</i> sp. Baird, 1845	52.6 \pm 75.2	59.1 \pm 48.8	18.8 \pm 34.9
<i>Chydorus</i> sp. Leach, 1816	16.2 \pm 20.0	5.4 \pm 7.1	0.3 \pm 0.9
Calanoids	8.7 \pm 9.3	17.3 \pm 12.9	947 \pm 1507
<i>Acartia longiremis</i> (Lilljeborg, 1853)	–	–	344 \pm 900
<i>Eurytemora affinis</i> (Poppe, 1880)	0.003 \pm 0.02	–	153 \pm 181
Cyclopoids	248 \pm 253	333 \pm 222	151 \pm 136
<i>Diacyclops thomasi</i> (S. A. Forbes, 1882)	12.1 \pm 13.5	14.4 \pm 13.2	10.1 \pm 11.2
<i>Eucyclops pectinifer</i> Cragin, 1883	1.3 \pm 2.6	0.04 \pm 0.1	–
Harpacticoids	6.9 \pm 8.0	6.6 \pm 4.8	462 \pm 641
<i>Nitokra hibernica</i> (Brady, 1880)	1.5 \pm 3.6	1.7 \pm 2.8	–
<i>Halectinosoma curticorne</i> (Boeck, 1872)	–	0.2 \pm 0.7	343 \pm 479
Total	346	429	1584
	Abundance		
	August		
	FSZ	FEZ	ETZ
	N=29	N=10	N=7
Cladocerans	149 \pm 342	49.1 \pm 50.4	31.6 \pm 68.7
<i>Bosmina</i> sp. Baird, 1845	75.7 \pm 219	24.9 \pm 28.3	26.9 \pm 63.2
<i>Chydorus</i> sp. Leach, 1816	12.7 \pm 62.0	1.8 \pm 2.2	–
Calanoids	89.4 \pm 210	188 \pm 159	1990 \pm 3408
<i>Acartia longiremis</i> (Lilljeborg, 1853)	–	–	23.4 \pm 29.9
<i>Eurytemora affinis</i> (Poppe, 1880)	4.0 \pm 7.3	16.2 \pm 15.8	709 \pm 1601
Cyclopoids	73.9 \pm 156	46.0 \pm 89.6	514 \pm 781
<i>Diacyclops thomasi</i> (S. A. Forbes, 1882)	0.1 \pm 0.3	–	–
<i>Eucyclops pectinifer</i> Cragin, 1883	29.6 \pm 144	2.3 \pm 4.9	–
<i>Halicyclops fosteri</i> M. S. Wilson, 1958	–	29.8 \pm 94.2	507 \pm 780
Harpacticoids	16.1 \pm 39.2	7.6 \pm 11.0	410 \pm 889
<i>Nitokra hibernica</i> (Brady, 1880)	3.4 \pm 4.1	1.3 \pm 1.9	0.1 \pm 0.3
<i>Halectinosoma curticorne</i> (Boeck, 1872)	–	–	391 \pm 847
Total	329	291	2946

very abundant in the ETZ and represented by a marine species (*Halectinosoma curticorne* (Boeck, 1872) (Fig. 4g–h). In the fluvial zones, we found benthic euryhaline (*Nitokra hibernica* (Brady, 1880) and *Onychocamptus mohammed* (Blanchard

and Richard, 1891) in August with *Mesochra alaskana* M.S. Wilson, 1958, *Schizopera borutzkyi* Monchenko, 1967) and freshwater (*Canthocamptus staphilinoides* Pearse, 1905 in May) species in low numbers.

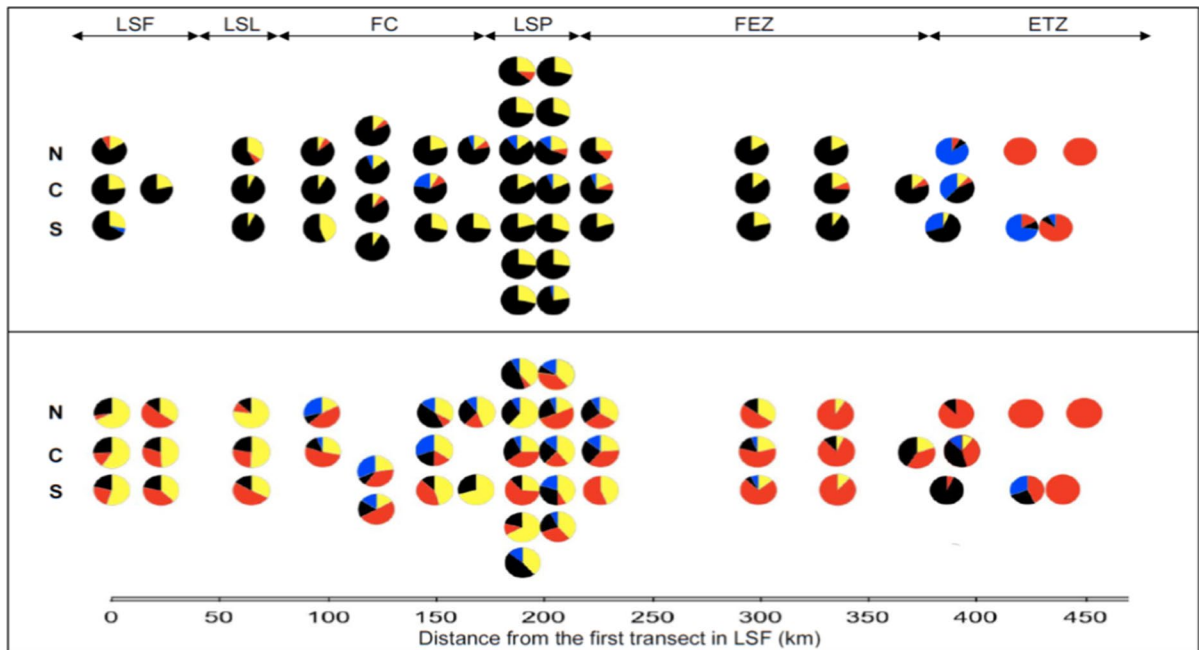


Fig. 3 Relative composition (pie charts) of the zooplankton community (major groups: cladocerans (yellow), calanoids (red), cyclopoids (black), harpacticoids (blue)) at each site, as a function of the distance (abscissa in km) from the westernmost transect in Lake Saint-François. Fluvial section zone abbreviations are shown at the top of the graph. Groups representing less than 5% of one site total abundance were not

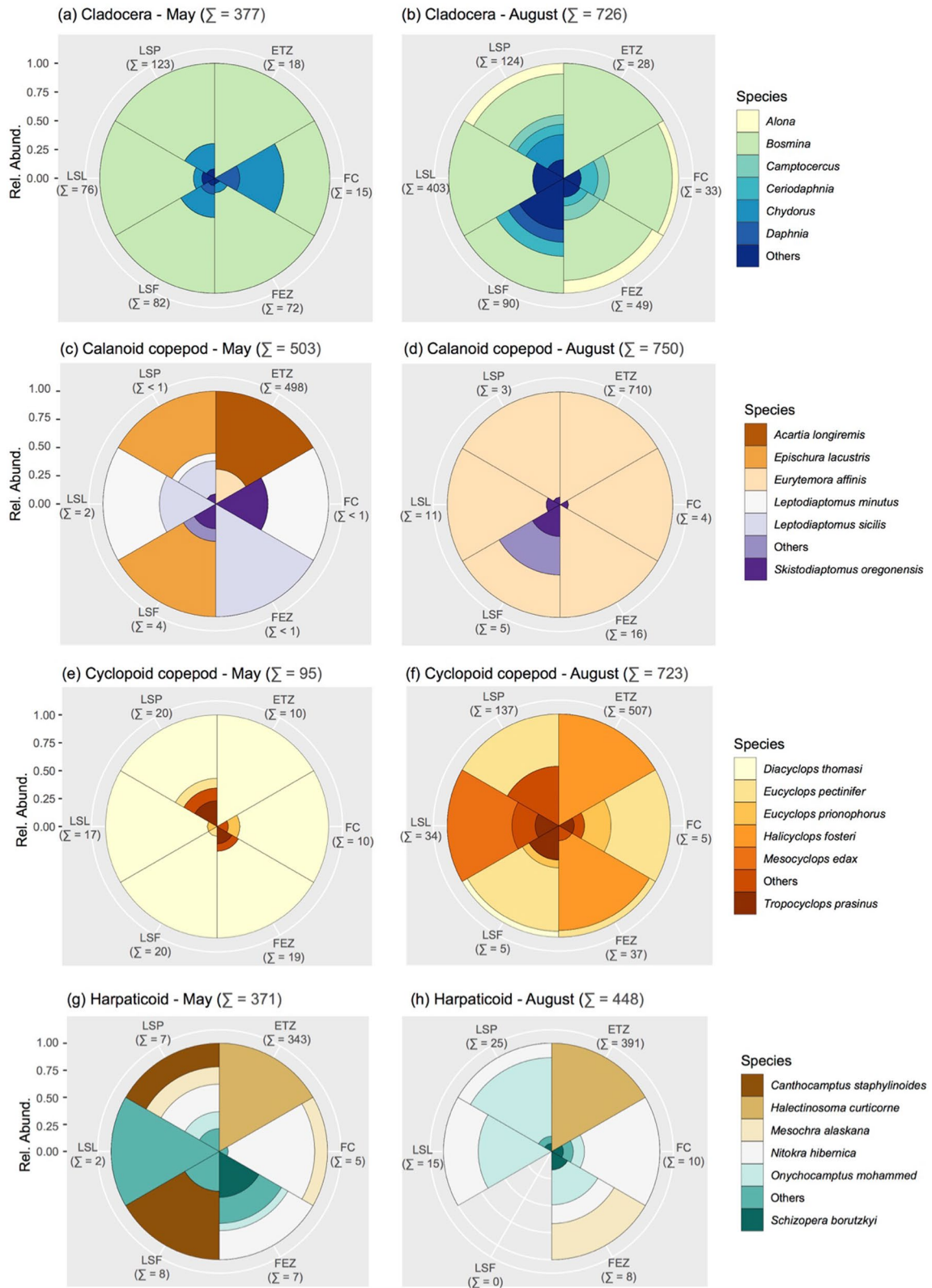
represented. *LSF* Lake Saint-François, *LSL* Lake Saint-Louis, *FC* Fluvial Corridor, *LSP* Lake Saint-Pierre, *FEZ* fluvial estuary zone, *ETZ*=Eetuarine transition zone. The letters N, C, and S to the left of the sites represent the northern, central and southern portions of the transects, respectively. Top panel: May; bottom panel: August

Spatial and environmental structures

Due to the clear and well-known dichotomy in zooplankton abundance and composition between the fluvial zones (FSZ, FEZ: sites 1–44) and the estuarine transition zone (ETZ: sites 46–52), further analyses solely examined the effects of hydrological networks (flow models) on the distribution of zooplankton groups in the fluvial zones, discarding all estuarine sites. Global RDAs were conducted using AEM eigenfunctions, with different transformations of the zooplankton data (Table S4, supplemental material). In May, the best model was ‘*Mixing without tributaries*’ with equal weights on the edges (‘*no weights on the edges*’) and log-chord transformation of the zooplankton data ($R^2_a=0.47$). In August, the model ‘*Mixing with tributaries*’ with equal weights on the edges and the Hellinger transformation gave the best R^2_a (0.61). However, another model ‘*No mixing with tributaries*’ with equal weights on edges resulted in a comparable R^2_a (0.60). The best combinations of

connection diagrams and zooplankton data transformation were submitted to forward selection of the AEM eigenfunctions in order to choose one best model-transformation for each hydroperiod (Table 3). Spatial patterns of distribution of zooplankton groups (cladocerans, calanoids, cyclopoids and harpacticoids) at each hydroperiod were illustrated using bubble plot maps of the fitted values of zooplankton data on the first two canonical axes of the best RDA models with selected AE model and transformation (Fig. S1, supplemental material).

The distribution of zooplankton groups at each hydroperiod in the fluvial zones indicated that there were more changes between hydroperiods than between zones (Fig. 3). However, spatially constrained clustering suggested that we can distinguish different groups of sites within each hydroperiod as well (Fig. 5). In May, we identified 10 groups, with group 1 representing a majority of the sites (22 of 44 sites, dark blue circles) located on the south shores in the fluvial lakes, corridor and estuary, whereas the



◀**Fig. 4** Rose diagrams describing zooplankton species composition for each crustacean group (Cladocerans, Calanoid Copepods, Cyclopoid Copepods, Harpacticoid Copepods) in May (a) and August (b), where distance of rays from centre represents relative abundances, while sums shown at the periphery indicate total abundance per site. *LSF* Lake Saint-François, *LSL* Lake Saint-Louis, *FC* Fluvial Corridor, *LSP* Lake Saint-Pierre, *FEZ* fluvial estuary zone, *ETZ* estuarine transition zone

other (smaller) groups comprised sites located on the north and south shores close to tributary confluences in the fluvial lakes (*LSF*, *LSL*, *LSP*) (Fig. 5a-c). However, despite minor changes in the relative abundance of zooplankton groups, most of the groups were dominated by cyclopoids. In August, we observed higher variation among the fluvial lakes and identified 11 groups (Fig. 5b-d). Groups 1-3 included sites from the first two fluvial lakes (*LSF* and *LSL*) whereas group 4 contained sites from the fluvial corridor (*FC*) and the third fluvial lake (*LSL*) as well as *FEZ* sites in the north shore; group 10 included *FEZ* sites in the south shore and the other groups were composed of sites close to tributary confluence in the north and south shores.

The relative influence of hydrological, spatial and environmental variables varied among hydroperiods (Fig. 6a-b). Forward selection retained some spatial variables in May and August (AEM, dbMEM), whereas environmental variables (ENV) were only retained in May. Seven AEMs, three dbMEMs and three environmental variables (turbidity, conductivity and TP) were selected in May, providing an R^2_a of 0.47 (Fig. 6c). Thirteen AEMs and six dbMEMs (but no environmental variables) were retained in August, producing an R^2_a of 0.61 (Fig. 6d). The resulting parsimonious RDA model for May explained 43% of the total variation in zooplankton community in the fluvial zones (Fig. 6a). The environmental variables (ENV) uniquely explained 9% of the variation, with an additional 11% co-explained by spatial processes (AEMs and dbMEMs) and the environmental conditions. Space (AEM and dbMEM, excluding all ENV variation) uniquely explained 23% of the remaining variation, 15% of which was due to the directional flow (AEM) while 3% was non-directional (dbMEM). Calanoid distribution was mostly related to upstream-downstream directional flow (AEM1, AEM16) while the other groups were influenced by both directional (AEMs) and non-directional (dbMEMs) flows (cyclopoids: AEM15, dbMEM8;

cladocerans: AEM7, dbMEM4; harpacticoids: AEM11, AEM6, dbMEM2) (Fig. 6c). The distribution of harpacticoids was also associated with higher turbidity, conductivity and nutrients (TP) (Fig. 6c). In August, the parsimonious RDA model explained 62% of the total variation in zooplankton community in the fluvial zones (Fig. 6b). The directional flow uniquely explained a bit more of the zooplankton variation (AEM: 11%) than the non-directional spatial influence (dbMEM: 6%), although most of the variation was jointly explained by both spatial models (45%). Copepod distribution was mostly related to directional flow (calanoids: AEM1, AEMs7-8, AEM14; cyclopoids: AEMs2-3, AEM8, AEMs1-12, AEM15, AEM18; harpacticoids: AEM1, AEM3, AEM5) while the cladocerans were associated to non-directional flow (dbMEM3) (Fig. 6d).

Discussion

Zooplankton distribution patterns along the fluvial estuarine continuum

Zooplankton distribution patterns in the SLR were primarily related to the longitudinal discontinuity in waters between the fluvial zones (*FSZ* and *FEZ*) and the estuarine transition zone (*ETZ*), and secondly to other longitudinal and transversal discontinuities in water masses within the fluvial lakes and corridor. As expected, fluvial and estuarine crustacean communities of the SLR differed in their species richness, abundance and composition, as previously reported for their biomass and functional diversity (Massicotte et al., 2014), and in other river-estuary macrosystems (Kim & Joo, 2000; Akopian et al., 2002; Tackx et al., 2004). Species richness was lower in the *ETZ* than in the fluvial zones (*FSZ* and *FEZ*), because only a few euryhaline copepods (calanoids and harpacticoids) can tolerate a wide range of salinities. In contrast, zooplankton abundance was much higher in the *ETZ* than in the fluvial zones because the powerful mixing of freshwater and marine waters in the *ETZ* causes the accumulation of phytoplankton, protists and euryhaline zooplankton, which proliferate in this nutrient-rich environment (Frenette et al., 1995; Barnard et al., 2003). The low abundance of crustacean zooplankton found in the fluvial zones is typical of other temperate rivers (Pace et al., 1992; Basu &

Table 3 R^2_a statistics of the best RDA analyses of the AEM models (without weights in all cases) with associated species data transformations (see Table S4 for results with weights on edges)

	AEM Models	Weights on edges	Transformations			
			Hellinger	Log-chord	Chord	Chi-square
May	Mixing with tributaries	no	0.328	0.407	0.041	0.390
	Mixing without tributaries	no	0.356	0.472	0.018	0.402
	No mixing with tributaries	no	0.297	0.375	0.017	0.404
	No mixing without tributaries	no	0.275	0.326	-0.008	0.362
August	Mixing with tributaries	no	0.610	0.583	0.593	0.484
	Mixing without tributaries	no	0.574	0.566	0.551	0.450
	No mixing with tributaries	no	0.600	0.564	0.571	0.463
	No mixing without tributaries	no	0.534	0.540	0.504	0.391

The highest R^2_a for each hydroperiod is in boldface

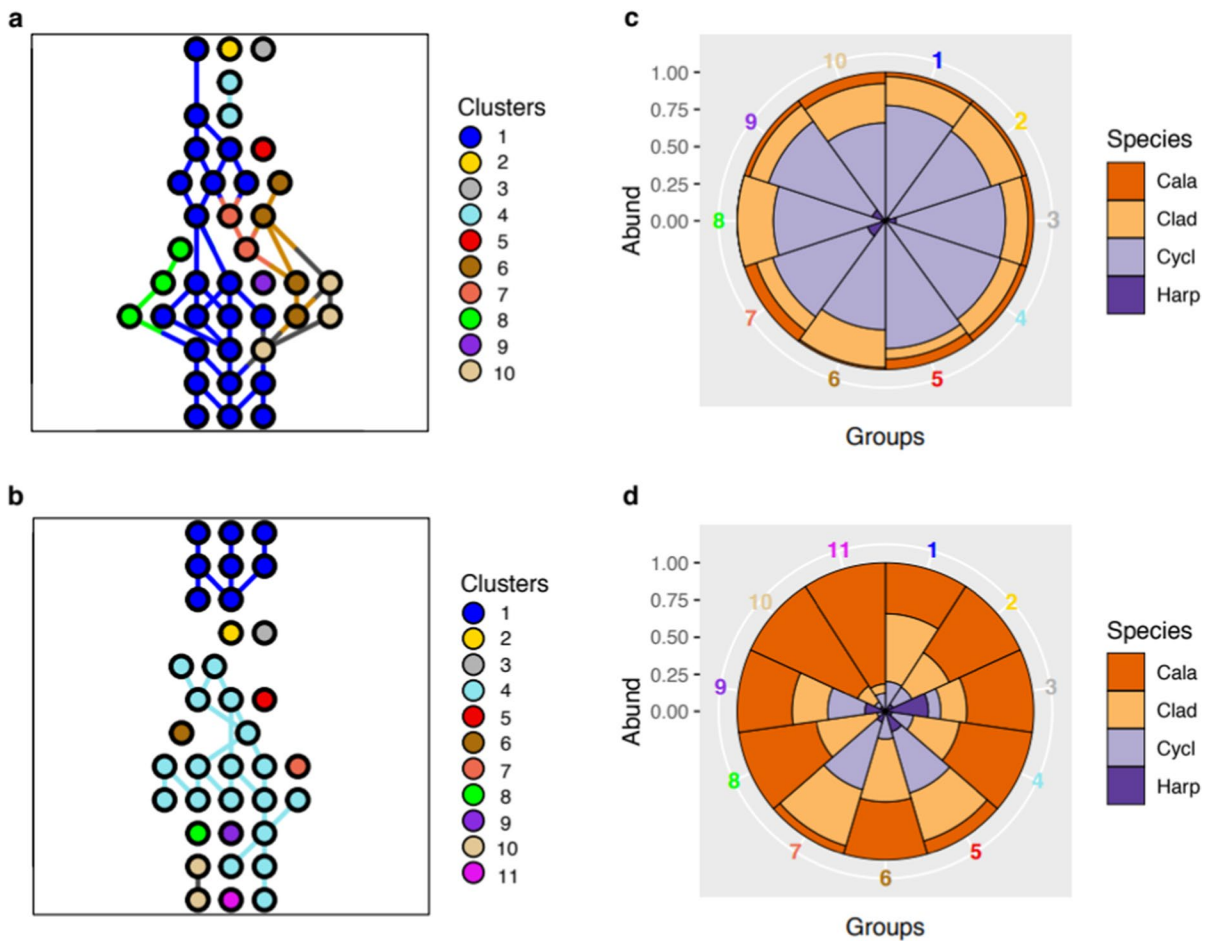


Fig. 5 Site clustering determined by spatially constrained clustering: **a** 10 groups in May, **b** 11 groups in August, based on the relative abundances of the four major zooplankton

groups. **c** and **d** rose diagrams of the taxonomic composition of the groups shown in (a) and (b)

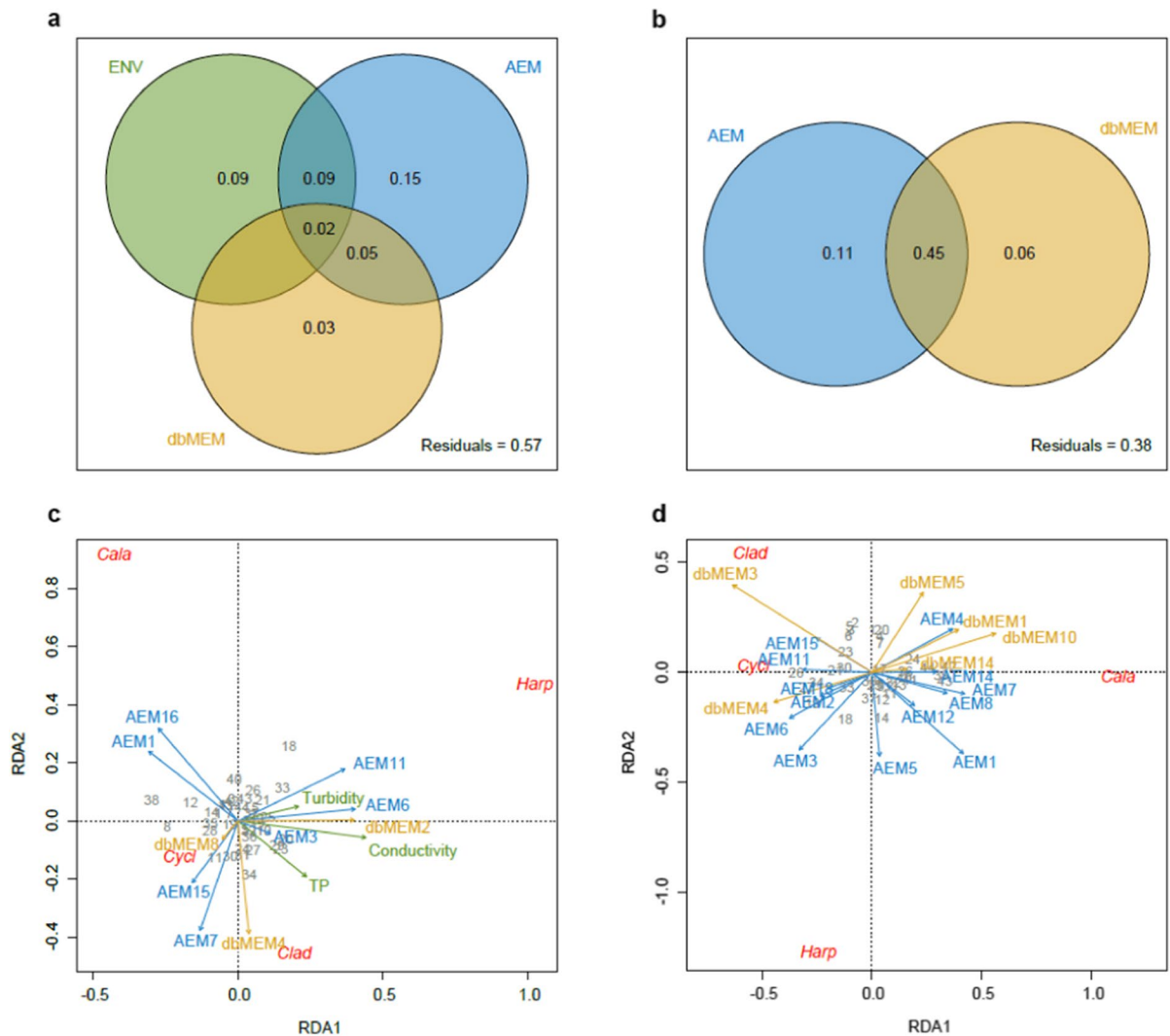


Fig. 6 Variation partitioning (top) and parsimonious RDA (bottom) results; (a, c) May and (b, d) August. RDA triplot showing the four taxonomic groups (abbreviations in red), the sites (numbers 1 to 44 in black), selected AEM flow variables (May: AEMs 1, 3, 6, 7, 11, 15, 16; August: AEMs 1 to

8, 11, 12, 14, 15, 18), non-directional dbMEM spatial variables (May: dbMEMs 2, 4, 7, 17; August: dbMEMs 1, 3, 5, 10, 14), and selected environmental variables (May: turbidity, total phosphorous, conductivity; August: none selected)

Pick, 1996; Basu et al. 2000a; Lair, 2006). However, fluvial lakes in the SLR act as zooplankton sources, since lower depth, slow-flowing-stagnant zones with high water residence times, as well as macrophyte littoral beds, favour the development of crustacean zooplankton (Basu et al., 2000b; Wetzel, 2001; Walks & St Cyr, 2004).

Overall, the cladocerans and copepods found in the SLR are typical of running waters (Dole-Olivier et al., 2000). They have diverse biological reproductive and

behavioural traits resulting in a great variety of life strategies that enable them to survive in lotic environments. Freshwater cladocerans were predominantly found in the fluvial zones, where the more extensive littoral zones, rich in submerged aquatic vegetation favoured this group (Bolduc et al., 2016, 2020). During both hydroperiods, cladocerans were largely represented by small species such as *Bosmina* and *Chydorus*, known to dominate the zooplankton community in most rivers of the world (Kobayashi et al.,

1998; Viroux, 1999; Kim & Joo, 2000; Tackx et al., 2004; Lair, 2006). Cladocerans were most abundant in August in the fluvial lake near Montreal (LSL). August also saw the appearance of littoral, macrophyte-associated taxa (*Alona* and *Camptocercus*; Wetzel, 2001; Bolduc et al., 2016, 2020) downstream of Montreal (FC, LSP, FEZ).

Calanoid copepods were most abundant as copepodid juvenile stages, as observed in other rivers (Poutriot et al., 1997; Kobayashi et al., 1998). In May, freshwater calanoids (*Leptodiptomus minutus*, *L. sicilis*, *Epischura lacustris*, *Skistodiptomus oregonensis*) were largely found in the fluvial zones (FSZ and FEZ), whereas euryhaline and marine species (*Acartia longiremis*, *Eurytemora affinis*) colonized the estuarine transition zone (ETZ). Surprisingly, the euryhaline species *Eurytemora affinis* was the dominant calanoid across the fluvial estuarine continuum in August. This species is a dominant planktonic and epibenthic grazer typically found in river estuaries and coastal bays in eastern North America (Aubé et al., 2005; Steinberg & Condon, 2009) and Europe (Tackx et al., 2004). Over the last century, *E. affinis* has invaded many freshwater habitats in rivers because it prefers low to medium salinity and can sustain strong and frequent salinity changes caused by mixing of fresh and saline waters (Lee, 1999; Lawrence et al., 2004; Michalec et al., 2010).

The occurrence of cyclopoid species within the fluvial zones in spring (notably *Diacyclops thomasi*) is likely due to their ability to survive as dormant stages in river backwaters (Wahl et al., 2008) and to emerge at spring (Napela, 1985; Hudson et al., 2003). In August, cyclopoids were much more diverse and abundant, and included benthic littoral species such as *Eucyclops pectinifer* and *E. prionophorus* as well as large species such as *Mesocyclops edax* which spend winter in diapause in the sediment until spring and mature in late summer (Selgeby, 1975). To our knowledge, *Halicyclops fosteri* was found for the first time in the fluvial estuarine zones (FEZ and ETZ) of the SLR (Pinel-Alloul et al., 2011). This euryhaline and benthic cyclopoid inhabits temperate estuaries such as the Delaware Bay (Aurand & Daiber, 1979) and the York River estuary (Steinberg & Condon, 2009).

Finally, freshwater species of harpacticoids were found in low numbers in the fluvial zones (relative to the estuarine zone), whereas euryhaline species were

more abundant in the estuarine transition zone. *Canthocamptus staphylinoides*, one of the most common harpacticoids in the Great Lakes (Robertson & Gannon, 1981), was reported in May in LSF and LSL, but disappeared in August probably because this species diapauses in late summer or early fall and encysts on the lake bottom (Nalepa, 1985). *Nitokra hibernica*, a species introduced to Lake Ontario (Czaika, 1978; Hudson et al., 2003) and commonly found along the weedy margins of large rivers and lakes, was found downstream in FC, LSL, and FEZ. By August, *N. hibernica* shared the dominance of the fluvial zone with *Onychocamptus mohammed*, a species distributed worldwide in fresh and saline inland waters and reported in the Great Lakes since 1990 (Hudson et al., 2003). *Schizopera borutzkyi*, likely introduced into the Great Lakes by ballast water exchange (Horvath et al., 2001), was largely found in the FEZ, whereas the euryhaline *Halectinosoma curticorne* species dominated the ETZ.

Linking zooplankton distribution to hydrological models and water mass environments

There are still few studies assessing directional and non-directional spatial forcing in freshwater and marine systems (Blanchet et al., 2011; Bertolo et al., 2012; Pollice et al., 2020), and none considering conjointly hydrological network and local environmental forcing. In the SLR, zooplankton distribution patterns did not follow a simple directional river model. Instead, discontinuities in water environment along the longitudinal (fluvial vs estuarine zones) and transversal (north vs south water masses) dimensions were conjointly shaping zooplankton distribution patterns in the SLR. The spatial forces influencing the distribution of zooplankton in the SLR are mainly influenced by directional flow networks (AEMs), as recently reported for zooplankton along a continuous waterscape in a large canyon reservoir (Rizo et al., 2020) and for macroinvertebrates in a river network (Pollice et al., 2020). However, the inclusion of non-directional spatial processes (dbMEMs) and local environmental conditions (ENV) produced a complete and informative model and improved our understanding of the changes between the spring and summer hydroperiods.

The type of flow models (i.e. whether mixing or tributaries were included) influenced zooplankton

distribution in the fluvial zones of the SLR, as they explained different portions of the total variation in zooplankton composition among sites both in May and August. In May, the zooplankton spatial pattern was best represented by the mixing model without tributaries likely due to the powerful effect of the flood that increased longitudinal directional processes and homogenization along the north and south shores. That is, removing the tributary links increased the proportion of explained variance by 7%; including lateral exchange between water masses (mixing) increased the variance explained by 15%, whereas hydrological processes (AEMs) accounted exclusively for 15% of total community variation. In August, we expected water masses to be well established and lateral exchanges between distinct water masses to be weak. Interestingly, we found that the two best models were mixing with tributaries and no mixing with tributaries. Thus, during this period of lower water levels, the input from tributaries seemed to be an important driver of zooplankton community composition. The increased importance of tributaries in August relative to May is evidenced by comparing the hydrological connection diagrams to the spatially constrained clustering results; in May we see that most sites belonged to a single cluster that ran across the river continuum (thus sites were largely homogeneous), whereas in August there was a notable change in community composition where tributary input became important, separating sites upstream and downstream of the Island of Montreal. The stability of the water mass distribution in August could also have reinforced this zooplankton distribution pattern relative to May where waters were more turbulent.

The type of weights on the edges was not important in either hydroperiods. Considering the exchanges among and within adjacent water masses as equally important was thus closer to reality than quantifying these exchanges by imperfect weights that represented different percentages of the original water masses. This suggests that discharge and water levels (May vs August) did not seem to impact the degree of exchange and mixing among the sites.

Transformations of zooplankton data greatly influenced the results in both hydroperiods. In May, the log-chord transformation gave the best results. This transformation is typically selected when there are a few very abundant and many rare species in a data matrix (Legendre & Borcard, 2018).

The $\log_e(y + 1)$ transformation greatly reduces the importance of the very abundant species, allowing the rare species to contribute to the dissimilarity measure, whereas the chord transformation that follows makes the dissimilarity measure double-zero asymmetrical, meaning that species absent from two sites do not change the dissimilarity between these sites. Indeed, when representing zooplankton groups in rose diagrams, we found that cyclopoids largely dominated the zooplankton community in May, whereas calanoids and harpacticoids were rare. In August, the Hellinger transformation, which reduces the importance of very abundant species without giving high weights to rare species (Legendre & Gallagher, 2001) led to the highest R^2_a . Thus, less abundant groups did not influence the results in the same way as in May. Indeed, differences between the mean abundance of zooplankton groups per site were much smaller in August than in May.

Selected AEM, dbMEM and environmental variables together explained 43% of the community variation in May whereas AEMs and dbMEMs alone explained 62% of the variation in August. The local water environment seemed therefore to have greater effect on the zooplankton distribution in May (10%) than in August (0%), during which zooplankton distribution seemed to be completely spatially structured and local environmental variables failed to explain an additional amount of the residual variation. These results agree with our first hypothesis predicting that zooplankton distribution patterns were more influenced by the water masses spatial structure than by local environmental factors. However, contrary to our second hypothesis, the spatial structure of the water masses explained more of the spatial zooplankton community variation in August than in May, whereas the effect of environmental factors was detectable in May but not in August. As noted above, strong currents and high discharge in May induced lateral mixing (i.e. the best RDA models contained mixing), leading to more homogeneous water masses, which may have allowed the SLR to behave more like a large lake where the effects of environmental conditions on the biota are felt. In August, slow-flowing water masses and lower water levels led to a stronger dependence on tributary inputs (i.e. the best RDA models included tributaries); thus, the well-separated water masses made the exchange of zooplankton

among sites more related to the effects of broader-scale water movements and masses.

Our results in August may have been affected by missing data. Unfortunately, some sites in the fluvial corridor and in Lake Saint-Pierre (LSP) were not sampled during the August cruise due to technical problems. The missing sites in LSP, which were located in the northern and southern littoral zones, were probably richer in zooplankton and their loss may have biased our results. This could also explain why total zooplankton abundance was lower in August than in May, where these sites were considered. Also, water current velocity, which was not measured during the cruises, would have been very useful to characterize the proximity between sites within a given water mass and would have allowed a simpler calculation of the possible exchanges between contiguous water masses.

Conclusion

This study is the first to have evaluated the effects of hydrological networks and environmental heterogeneity on zooplankton communities across the fluvial to estuary continuum of the St. Lawrence River. In doing so, we found evidence that directional flow patterns are the most influential in this continuous riverscape. However, non-directional flow patterns and environmental factors complement each other in shaping crustacean zooplankton distributions. Our use of directional spatial eigenfunctions (AEMs) supported the hypothesis that hydrological dynamics played a major role in structuring zooplankton communities. First, the longitudinal discontinuity between the fluvial and estuarine water masses had a clear influence on crustacean zooplankton richness, abundance and composition. Furthermore, within the fluvial zone, the water flow network caused by both directional (longitudinal) and non-directional (transversal) discontinuities in water masses among and within the fluvial lakes significantly regulated zooplankton abundance and composition. We also noted important changes in zooplankton composition among the two hydroperiods (spring and summer), which can be attributed to life-history and ecological adaptations of certain groups, notably copepods (emergence from diapause and development at spring) and cladocerans (dominance during summer due to the presence of favourable vegetated habitats). Water environment

also affected zooplankton community structure, notably nutrients (total phosphorus), conductivity and turbidity. Taken together, we believe that the methods presented herein may help in tracking changes in the composition of zooplankton and other trophic level organisms in the face of ongoing losses in macrophyte beds in the SLR fluvial lakes, combined with the predicted rise in water levels, nutrient levels, invasive species and changes in hydrology.

Acknowledgements This study was partially supported by grants from the Natural Science and Engineering Research Council (NSERC to BPA: 04875 and to PL: 7738) and the Fonds Québécois de la Recherche sur la Nature et les Technologies (FQRNT to the GRIL: RS-203279). The sampling cruises were carried on the *Lampsilis* vessel of the GRIL and supported by a grant from the NSERC ship time program. We thank the Captain F. Harvey and the crew of the *Lampsilis* vessel and assistants (Simon de Sousa, Patrice Thibeault, Virginie Roy and Ginette Méthot) for their invaluable support during cruises and field sampling. We are particularly indebted to Ginette Méthot (Université de Montréal) for helping in zooplankton taxonomic analysis, to Olivier Champoux and Jean Morin (ECCC) for the mapping of water masses, to Conrad Beauvais and Maude Lachapelle (ECCC) for the final composition of the Figure 1 and references and to Guillaume Blanchet for help with the AEM statistical analyses. This paper is a contribution of the GRIL research group of Université de Montréal to a special issue of *Hydrobiologia* in honour of Professor Henri Dumont.

Funding NSERC, 04875, Pinel–Alloul Bernadette, 7738, Pierre Legendre

Data availability The datasets generated during and/or analysed during the current study are not publicly available but are available on demand and presented in supplementary material.

Declarations

Conflict of interest The authors declare that they have no conflict of interest.

References

- Akopian, M., J. Garnier & R. Pourriot, 2002. Cinétique du zooplancton dans un continuum aquatique: de la Marne et son réservoir à l'estuaire de la Seine. *C.R. Biologie* 305: 807–818. [https://doi.org/10.1016/S1631-0691\(02\)01483-X](https://doi.org/10.1016/S1631-0691(02)01483-X).
- Amoros, C., 1984. Introduction pratique à la systématique des eaux continentales françaises. 5. Crustacés Cladocères. Association Française de Limnologie, Paris <https://doi.org/10.3406/linly.1984.10627>
- American Public Health Association (A.P.H.A.), 1998. Standard methods for the examination of water and wastewater, APHA, Washington, DC. ISBN 0875532357

- Aubé, C. I., A. Locke & G. J. Klassen, 2005. Zooplankton communities of a dammed Estuary in the Bay of Fundy, Canada. *Hydrobiologia* 548: 127–139. <https://doi.org/10.1007/s10750-005-4730-0>.
- Aurand, D. & F. C. Daiber, 1979. Further observations on the occurrence of *Halicyclops fosteri* Wilson (Copepoda, Cyclopoida) in the Delaware Bay region, USA. *Crustaceana* 36: 155–165. <https://doi.org/10.1163/156854079X00348>.
- Balcer, M. D., N. L. Korda & S. I. Dodson, 1984. Zooplankton of the Great Lakes: A guide to the identification and Ecology of the common crustacean species. The University of Wisconsin Press, Wisconsin. ISBN 0-299-09820-6.
- Baranyi, C., T. Hein, C. Holarek, S. Keckeis & F. Schimer, 2002. Zooplankton biomass and community structure in a Danube River Floodplain system: effects of hydrology. *Freshwater Biology* 47: 473–482. <https://doi.org/10.1046/j.1365-2427.2002.00822.x>.
- Barnard, C., J. J. Frenette & W. Vincent, 2003. Planktonic invaders of the St. Lawrence estuarine transition zone: environmental factors controlling the distribution of zebra mussel veligers. *Canadian Journal of Fisheries and Aquatic Sciences* 60: 1245–1257. <https://doi.org/10.1139/f03-103>.
- Basu, B. K. & F. R. Pick, 1996. Factors regulating phytoplankton and zooplankton biomass in temperate rivers. *Limnology and Oceanography* 41: 1572–1577. <https://doi.org/10.4319/lo.1996.41.7.1572>.
- Basu, B. K. & F. R. Pick, 1997. Phytoplankton and zooplankton development in a lowland, temperate river. *Journal of Plankton Research* 19: 237–253. <https://doi.org/10.1093/plankt/19.2.237>.
- Basu, B. K., J. Kalf & B. Pinel-Alloul, 2000a. Mid-summer plankton development along a large temperate river: The St. Lawrence River. *Canadian Journal of Fisheries and Aquatic Sciences* 57(Suppl. 1): 7–15. <https://doi.org/10.1139/f99-249>.
- Basu, B. K., J. Kalf & B. Pinel-Alloul, 2000b. The influence of macrophyte beds on plankton communities and their export from fluvial lakes in the St Lawrence River. *Freshwater Biology* 45: 373–382. <https://doi.org/10.1046/j.1365-2427.2000.00635.x>.
- Bertolo, A., F. G. Blanchet, P. Magnan, P. Brodeur, M. Mingelbier & P. Legendre, 2012. Inferring processes from spatial patterns: The role of directional and non-directional forces in shaping fish larvae distribution in a freshwater lake system. *PLoS ONE* 7(11): e50239. <https://doi.org/10.1371/journal.pone.0050239>.
- Blanchet, F. G., P. Legendre & D. Borcard, 2008a. Modelling directional spatial processes in ecological data. *Ecological Modelling* 215: 325–336. <https://doi.org/10.1016/j.ecolmodel.2008.04.001>.
- Blanchet, F. G., P. Legendre & D. Borcard, 2008b. Forward selection of explanatory variables. *Ecology* 89: 2623–2632. <https://doi.org/10.1890/07-0986.1>.
- Blanchet, F. G., P. Legendre, R. Maranger, D. Monti & P. Pepin, 2011. Modelling the effect of directional spatial ecological processes at different scales. *Oecologia* 166: 357–368. <https://doi.org/10.1007/s00442-010-1867-y>.
- Bolduc, P., A. Bertolo, C. Hudon & B. Pinel-Alloul, 2020. Submerged aquatic vegetation cover and complexity drive crustacean zooplankton community structure in a large fluvial lake: An *in situ* approach. *Journal of Great Lakes Research* 46: 767–779. <https://doi.org/10.1016/j.jglr.2019.12.011>.
- Bolduc, P., A. Bertolo & B. Pinel-Alloul, 2016. Does submerged aquatic vegetation shape zooplankton community structure and functional diversity? A test with a shallow fluvial lake system. *Hydrobiologia* 778: 151–165. <https://doi.org/10.1007/s10750-016-2663-4>.
- Borcard, D. & P. Legendre, 2002. All-scale spatial analysis of ecological data by means of principal coordinates of neighbour matrices. *Ecological Modelling* 153: 51–68. [https://doi.org/10.1016/S0304-3800\(01\)00501-4](https://doi.org/10.1016/S0304-3800(01)00501-4).
- Borcard, D., P. Legendre & P. Drapeau, 1992. Partialling out the spatial component of ecological variation. *Ecology* 73: 1045–1055. <https://doi.org/10.2307/1940179>.
- Borcard, D., F. Gillet & P. Legendre, 2018. Numerical ecology with R, 2nd edition. Use R! series, Springer International Publishing AG. ISBN: 978-3-319-71404-2
- Burdiss, R. M. & R. J. H. Hoxmeier, 2011. Seasonal zooplankton dynamics in main channel and backwater habitats of the Upper Mississippi River. *Hydrobiologia* 667: 69–87. <https://doi.org/10.1007/s10750-011-0639-y>.
- Casper, A. F. & J. H. Thorp, 2007. Diel and lateral patterns of zooplankton distribution in the St Lawrence River. *River Research and Applications* 23: 73–85. <https://doi.org/10.1002/rra.966>.
- Centre Saint-Laurent – CSL, 1996. Rapport-synthèse sur l'état du Saint-Laurent. Volume 1 : L'écosystème du Saint-Laurent. Environnement Canada – Région du Québec, Conservation de l'environnement – et Éditions Multi Mondes, Montréal. Coll. « BILAN Saint-Laurent. ISBN 2–921146–26–6
- Champoux, O. & J. Morin, 2007. Use of 2D convection-diffusion model in habitat modelling of the St Lawrence River, Canada. Environment Canada, Meteorological Service of Canada, Québec, Canada.
- Czaika, S. C., 1978. Crustacean zooplankton of southwestern Lake Ontario in spring 1973 and at the Niagara and Genesee River mouth areas in 1972 and spring 1973. *Journal of Great Lakes Research* 4: 1–9. [https://doi.org/10.1016/S0380-1330\(78\)72159-3](https://doi.org/10.1016/S0380-1330(78)72159-3).
- Dickerson, K. D., K. A. Medley & J. E. Havel, 2010. Spatial variation in zooplankton community structure is related to hydrological flow units in the Missouri River, USA. *River Research and Applications* 26: 605–618. <https://doi.org/10.1002/rra.1268>.
- Dole-Olivier, M.-J., D. M. P. Galassi, P. Marmonier & M. Cruzé des Chateliers, 2000. The biology and ecology of lotic microcrustaceans. *Freshwater Biology* 44: 63–91. <https://doi.org/10.1046/j.1365-2427.2000.00590.x>.
- Doretto, A., E. Piano & C. E. Larson, 2020. The River Continuum Concept: lessons from the past and perspectives for the future. *Canadian Journal of Fisheries and Aquatic Sciences* 77: 1853–1864. <https://doi.org/10.1139/cjfas-2020-0039>.
- Dray, S., D. Bauman, G. Blanchet, D. Borcard, S. Clappe, G. Guénard, T. Jombart, G. Larocque, P. Legendre, N. Madi & H. H. Wagner, 2022. adespacial: Multivariate multiscale spatial analysis. R package version 0.3–16. [available on internet at <https://cran.r-project.org/package=adespatial>]

- Edmonston, W. T., 1959. Fresh-water Biology. John Wiley & Sons, Inc., New York. ISBN 047123298.
- Frenette, J. J., W. F. Vincent, J. J. Dodson & C. Lovejoy, 1995. Size-dependent variations in phytoplankton and protozoan community structure across the St. Lawrence River transition region. *Marine Ecology Progress Series* 120: 99–110. <https://doi.org/10.3354/meps120099>.
- Frenette, J. J., M. T. Arts, J. Morin, D. Gratton & C. Martin, 2006. Hydrodynamic control of the underwater light climate in fluvial Lac Saint-Pierre. *Limnology and Oceanography* 51: 2632–2645. <https://doi.org/10.4319/lo.2006.51.6.2632>.
- Guénard, G. & P. Legendre, 2022. Hierarchical clustering with contiguity constraint in R. *Journal of Statistical Software* 103(7): 1–26. <https://doi.org/10.18637/jss.v103.i07>.
- Havel, J. E., K. A. Medley, K. D. Dickerson, T. R. Angradi, D. W. Bolgrien, P. A. Bukaveckas & T. M. Jicha, 2009. Effect of main-stem dams on zooplankton communities of the Missouri River (USA). *Hydrobiologia* 628: 121–135. <https://doi.org/10.1007/s10750-009-9750-8>.
- Hebert, P. D. N., 1995. The *Daphnia* of North America: An Illustrated Fauna, University of Guelph, CD-ROM:
- Horvath, T. G., R. L. Whitman & L. L. Last, 2001. Establishment of two invasive crustaceans (Copepoda, Harpacticoida) in the nearshore sands of Lake Michigan. *Canadian Journal of Fisheries and Aquatic Sciences* 58: 1261–1264. <https://doi.org/10.1139/cjfas-58-7-1261>.
- Hudon, C., 1997. Impact of water level fluctuations on St. Lawrence River aquatic vegetation. *Canadian Journal of Fisheries and Aquatic Sciences* 54: 2853–2865. <https://doi.org/10.1139/f97-201>.
- Hudson, P. L., L. T. Lesko, J. W. Reid & M. A. Chriscinske, 2003. Cyclopoid copepods of the Laurentian Great Lakes. Ann Arbor, MI: Great Lakes Science Center Home Page. [available on internet at <http://www.glsc.usgs.gov/greatlakescopepods/Key.asp?GROUP=Cyclopoid>] Accessed 2009.
- Humphries, P., H. Keckeis & R. Findlayson, 2014. The river wave concept: integrating river ecosystem models. *Bioscience* 64: 870–882. <https://doi.org/10.1093/biosci/biu130>.
- Huys, R., J. M. Gee, G. G. Moore & R. Hamond, 1996. Marine and brackish water harpacticoid copepods. Field Studies Council, Shrewsbury, England. ISBN 1851532560
- Junk, W. J., P. B. Bayley & R. E. Sparks, 1989. The flood pulse concept in river floodplain systems. *Canadian Special Publication of Fisheries and Aquatic Sciences* 106: 110–127.
- Kim, H. W. & J. J. G. Joo, 2000. The longitudinal distribution and community dynamics of zooplankton in a regulated large river: a case study of the Nakdong River (Korea). *Hydrobiologia* 438: 171–184. <https://doi.org/10.1023/A:1004185216043>.
- Kobayashi, T., R. J. Shiel, P. Gibbs & P. I. Dixon, 1998. Fresh-water zooplankton in the Hawkesbury-Nepean River: comparison of community structure with other rivers. *Hydrobiologia* 377: 133–145. <https://doi.org/10.1023/A:1003240511366>.
- Lacroix, G., 1981. Guide d'identification du zooplancton: Estuaire et golfe du Saint-Laurent, Université Laval, Département de biologie, Québec:
- Lair, N., 2006. A review of regulation mechanisms of meta-zoan plankton in riverine ecosystems: aquatic habitat versus biota. *River Research and Applications* 22: 567–593. <https://doi.org/10.1002/rra.923>.
- Lawrence, D., I. Valiela & G. Tomasky, 2004. Estuarine calanoid copepod abundance in relation with season, salinity, and land-derived nitrogen loading, Waquoit Bay, MA. *Estuarine Coastal Maine Research* 61: 547–557. <https://doi.org/10.1016/j.ecss.2004.06.018>.
- Le Coz, M., S. Chambord, P. Meire, T. Maris, F. Azémar, J. Ovaert, E. Buffan-Dubau, J. C. Kromkamp, A. C. Sossou, J. Prygiel, G. Spronk, S. Lamothe, B. Ouddane, S. Rabodonirina, S. Net, D. Dumoulin, J. Peene, S. Souissi & M. Tackx, 2017. Test of some ecological concepts on the longitudinal distribution of zooplankton along a lowland water course. *Hydrobiologia* 802: 175–198. <https://doi.org/10.1007/s10750-017-3256-6>.
- Lee, C. E., 1999. Rapid and repeated invasions of fresh water by the saltwater copepod *Eurytemora affinis*. *Evolution* 53: 1423–1434. <https://doi.org/10.1111/j.1558-5646.1999.tb05407.x>.
- Legendre, P. & D. Borcard, 2018. Box-Cox-chord transformations for community composition data prior to beta diversity analysis. *Ecography* 41: 1820–1824. <https://doi.org/10.1111/ecog.03498>.
- Legendre, P. & E. D. Gallagher, 2001. Ecological meaningful transformations for ordination of species data. *Oecologia* 129: 271–280. <https://doi.org/10.1007/s004420100716>.
- Legendre, P. & L. Legendre, 2012. Numerical ecology, 3rd English edition. Elsevier, Amsterdam, The Netherlands. ISBN: 978-0-444-53868-0.
- Lesko, L. T., P. L. Hudson & M. A. Chriscinske, 2003a. Calanoid copepods of the Laurentian Great Lakes. Ann Arbor, MI: Great Lakes Science Center Home Page. [available on internet at <http://www.glsc.usgs.gov/greatlakescopepods/Key.asp?GROUP=Calanoid>]
- Lesko, L. T., P. L. Hudson, J. W. Reid & M. A. Chriscinske, 2003b. Harpacticoid copepods of the Laurentian Great Lakes. Ann Arbor, MI: Great Lakes Science Center Home Page. [available on internet at <http://www.glsc.usgs.gov/greatlakescopepods/Key.asp?GROUP=Harpacticoid>]
- Massicotte, P. & J. J. Frenette, 2011. Spatial connectivity in a large river system: resolving the sources and fate of dissolved organic matter. *Ecological Applications* 21: 2600–2617. <https://doi.org/10.1890/10-1475.1>.
- Massicotte, P., J. J. Frenette, R. Proulx, B. Pinel-Alloul & A. Bertolo, 2014. Riverscape heterogeneity explains spatial variation in zooplankton functional evenness and biomass in a large river ecosystem. *Landscape Ecology* 29: 67–79. <https://doi.org/10.1007/s10980-013-9946-1>.
- McCluney, K. E., N. Le Roy Poff, M. A. Palmer, J. H. Thorp, G. C. Poole, B. S. Williams, M. R. Williams & J. S. Baron, 2014. Riverine macrosystems ecology: sensitivity, and resilience of whole river basins with human alterations. *Frontiers in Ecology and Environment* 12: 48–58. <https://doi.org/10.1890/120367>.
- Michalec, F. G., S. Souissi, G. Dur, M. S. Mahjoub, F. G. Schmitt & J. S. Hwang, 2010. Differences in behaviour responses of *Eurytemora affinis* (Copepoda, Calanoida) reproductive stages to salinity variations. *Journal of*

- Plankton Research 32: 805–813. <https://doi.org/10.1093/plankt/fbq006>.
- Mills, E. L., S. B. Smith & J. L. Forney, 1981. The St. Lawrence River in winter: population structure, biomass and pattern of its primary and secondary food web components. *Hydrobiologia* 79: 65–75. <https://doi.org/10.1007/BF00005820>.
- Napela, N. F., 1985. Occurrence of a resting stage in cyclopoid and harpacticoid copepods in nearshore Lake Michigan. *Journal of Great Lakes Research* 11: 59–66. [https://doi.org/10.1016/S0380-1330\(85\)71744-3](https://doi.org/10.1016/S0380-1330(85)71744-3).
- Oksanen, J., G. L. Simpson, G. Blanchet, R. Kindt, P. Legendre, P. R. Minchin, R. B. O'Hara, P. Solymos, M. H. H. Stevens, E. Szoecs & H. Wagner, 2022. *vegan: Community Ecology Package*. R package version 2.6-2. [available on internet at <https://github.com/vegandevs/vegan>]
- Pace, M., S. Findlay & D. Lints, 1992. Zooplankton in advective environments: the Hudson River community and a comparative analysis. *Canadian Journal of Fisheries and Aquatic Sciences* 49: 1060–1069. <https://doi.org/10.1139/f92-117>.
- Parsons, T. R., Y. Maita & C. M. Lalli, 1984. A manual of chemical and biological methods for seawater analysis. Pergamon Press, Toronto. ISBN 978-0-08-030287-4
- Picard, V. & N. Lair, 2005. Spatio-temporal investigations on the planktonic organisms of the Middle Loire (France), during the low water period: biodiversity and community dynamics. *Hydrobiologia* 551: 68–86. <https://doi.org/10.1007/s10750-005-4451-4>.
- Pinel-Alloul, B., E. Cusson & L. Aldamman, 2011. Diversity and spatial distribution of copepods in the St. Lawrence River (Québec, Canada). *Crustaceana Monographs*. 16: 425–429. <https://doi.org/10.1163/9789004188280-020>.
- Pollice, A., G. Jona-Lasinio, M. Gaglio, F. G. Blanchet & E. A. Fano, 2020. Modelling the effect of directional spatial ecological processes for a river network in Northern Italy. *Ecological Indicators* 112: 106144. <https://doi.org/10.1016/j.ecolind.2020.106144>.
- Pourriot, R., C. Rougier & A. Miquelis, 1997. Origin and development of river zooplankton: example of the Marne. *Hydrobiologia* 345: 143–148. <https://doi.org/10.1023/A:1002935807795>.
- Prepas, E. E., 1978. Sugar-frosted *Daphnia*: An improved fixation technique for Cladocera. *Limnology and Oceanography* 23: 557–559. <https://doi.org/10.4319/lo.1978.23.3.0557>.
- R Development Core Team, 2022. R: A language and environment for statistical computing. R Foundation for Statistical Computing, Vienna, Austria.
- Rizo, E. Z. C., P. Liu, H. Niu, Y. Yang, Q. Lin, H. J. Dumont & B.-P. Han, 2020. Zooplankton in a continuous waterscape: Environmental and spatial factors shaping spring zooplankton community structure in a large canyon reservoir at the tropic of cancer. *Hydrobiologia* 847: 3621–3635. <https://doi.org/10.1007/s10750-020-04380-1>.
- Robertson, A. & J. E. Gannon, 1981. Annotated checklist of the free-living copepods of the Great Lakes. *Journal of Great Lakes Research* 7: 382–393. [https://doi.org/10.1016/S0380-1330\(81\)72066-5](https://doi.org/10.1016/S0380-1330(81)72066-5).
- Rozon, R. M., K. L. Bowen, H. A. Niblock, M. A. J. Fitzpatrick & W. A. J. Currie, 2016. Assessment of the phytoplankton and zooplankton populations in the Niagara River (Canada) Area of Concern in 2014. Canadian Technical Report of Fisheries and Aquatic Sciences 3184: iv + 66p. ISBN 978-0-660-06792-6
- Selgeby, J. H., 1975. Life histories and abundance of crustacean zooplankton in the outlet of Lake Superior, 1971–1972. *Journal of Fisheries Research Board of Canada* 32: 461–470. <https://doi.org/10.1139/f75-056>.
- Simons, R. D., S. G. Monismith, L. E. Johnson, G. Winkler & F. J. Saucier, 2006. Zooplankton retention in the estuarine transition zone of the St Lawrence Estuary. *Limnology and Oceanography* 51: 2006–2621. <https://doi.org/10.4319/lo.2006.51.6.2621>.
- Smith, K. & C. H. Fernando, 1978. A guide to freshwater calanoid and cyclopoid copepod crustacea of Ontario, University of Waterloo Biology series, Ontario:
- Stanford, J. A. & J. V. Ward, 2001. Revisiting the serial discontinuity concept. *Regulated Rivers: Research and Management* 17: 303–310. <https://doi.org/10.1002/rrr.659>.
- Steinberg, D. K. & R. H. Condon, 2009. Zooplankton of the York River. *Journal of Coastal Research* 57: 66–79. <https://doi.org/10.2112/1551-5036-57.sp1.66>.
- Tackx, M. L. M., N. De Pawn, R. Van Meighem, F. Azémar, A. Hannouti, S. Van Damme, F. Fiers, N. Daro & P. Meire, 2004. Zooplankton in the Schelde Estuary, Belgium and the Netherlands. Spatial and temporal patterns. *Journal of Plankton Research* 26: 133–141. <https://doi.org/10.1093/plankt/fbh016>.
- Thorp, J. H. & A. F. Casper, 2003. Importance of biotic interactions in large rivers: An experiment with planktivorous fish, dreissenid mussels and zooplankton in the St Lawrence River. *River Research and Applications* 19: 265–279. <https://doi.org/10.1002/rra.703>.
- Thorp, J. H. & M. D. Delong, 1994. The Riverine Productivity Model: a heuristic view of carbon sources and organic processing in large river ecosystems. *Oikos* 70: 305–308. <https://doi.org/10.2307/3545642>.
- Thorp, J. H., A. R. Black, K. H. Haag & J. D. Wehr, 1994. Zooplankton assemblages in the Ohio River: seasonal, tributary, and navigation dam effects. *Canadian Journal of Fisheries and Aquatic Sciences* 51: 1634–1643. <https://doi.org/10.1139/f94-164>.
- Thorp, J. H., M. C. Thoms & M. D. Delong, 2006. The riverine ecosystem synthesis: biocomplexity in river networks across space and time. *River Research Applications* 22: 123–147. <https://doi.org/10.1002/rra.901>.
- Thorp, J. H., M. C. Thoms & M. D. Delong, 2008. The riverine ecosystem synthesis: Towards conceptual cohesiveness in river science. Academic Press: London, UK, 232p. ISBN: 978-0-12-370612-6
- Tockner, K., F. Malard & J. V. Ward, 2000. An extension of the flood pulse concept. *Hydrological Processes*. 14: 2861–2883. [https://doi.org/10.1002/1099-1085\(200011/12\)14:16/17%3c2861::AID-HYP124%3e3.0.CO;2-F](https://doi.org/10.1002/1099-1085(200011/12)14:16/17%3c2861::AID-HYP124%3e3.0.CO;2-F).
- Twiss, M. R., C. Ulrich, S. A. Kring, J. Harold & M. Williams, 2010. Plankton dynamics along a 180 km reach of the Saint Lawrence River from its headwaters in Lake Ontario. *Hydrobiologia* 647: 7–20. <https://doi.org/10.1007/s10750-010-0115-0>.
- Vannote, R., G. Minshall, K. Cummins, J. Sedell & C. Cushing, 1980. The River Continuum Concept. *Canadian Journal of*

- Fisheries and Aquatic Sciences 37: 130–137. <https://doi.org/10.1139/f80-017>.
- Viroux, L., 1997. Zooplankton development in two large lowland rivers, the Moselle (France) and the Meuse (Belgium), in 1993. *Journal of Plankton Research* 19: 1743–1762. <https://doi.org/10.1093/plankt/19.11.1743>.
- Viroux, L., 1999. Zooplankton distribution in flowing waters and its implications for sampling: case studies in the River Meuse (Belgium) and the River Moselle (France, Luxembourg). *Journal of Plankton Research* 21: 1231–1248. <https://doi.org/10.1093/plankt/21.7.1231>.
- Wahl, D. H., J. Goodrich, M. A. Nannini, J. M. Dettmers & D. A. Soluk, 2008. Exploring riverine zooplankton in three habitats of the Illinois River ecosystem: Where do they come from? *Limnology and Oceanography* 53: 2583–2593. <https://doi.org/10.4319/lo.2008.53.6.2583>.
- Walks, D. & H. Cyr, 2004. Movement of plankton through lake-stream systems. *Freshwater Biology* 49: 745–759. <https://doi.org/10.1111/j.1365-2427.2004.01220.x>.
- Walkusz, W., J. E. Paulić, S. Kwaśniewski, W. J. Williams, S. Wong & M. H. Papst, 2010. Distribution, diversity and biomass of summer zooplankton from the coastal Canadian Beaufort Sea. *Polar Biology* 33: 321–335. <https://doi.org/10.1007/s00300-009-0708-0>.
- Ward, J., 1995. A description of new zooplankton counter. *Quarterly Journal of Microscopical Science* 96: 371–373. <https://doi.org/10.1242/jcs.s3-96.35.371>.
- Ward, J. & J. Stanford, 1983. The serial discontinuity concept of lotic ecosystems. In Fontaine, T. D. B. S. (ed), *Dynamics of Lotic Ecosystems* Ann Arbor Scientific Publishers, Ann Arbor: 29–42.
- Wetzel, R., editor. 2001. *Limnology : lake and river ecosystems* San Diego, Calif.: London: Academic, c2001. ISBN-13: 978-0-12-744760-5
- Winkler, G., J. J. Dodson, N. Bertrand, D. Thivierge & W. F. Vincent, 2003. Trophic coupling across the St. Lawrence River estuarine transition zone. *Marine Ecology Progress Series* 251: 59–73. <https://doi.org/10.3354/meps251059>.

Publisher's Note Springer Nature remains neutral with regard to jurisdictional claims in published maps and institutional affiliations.

Springer Nature or its licensor (e.g. a society or other partner) holds exclusive rights to this article under a publishing agreement with the author(s) or other rightsholder(s); author self-archiving of the accepted manuscript version of this article is solely governed by the terms of such publishing agreement and applicable law.

Supplemental material – HYDR-D-22-00651-R2

Table S1. Mix of water masses at each sampling sites on the days of sampling (May 23rd to 30th, August 8th to 15th). The water mass column shows the proportion of each water mass present at the sites: Great Lakes (GL), south shore channel (CRS), Ottawa River (OTT), the Mille Îles and des Prairies Rivers (MIP), Richelieu River (RICH), Maskinongé River (MASK) and waters of the Québec City Region (QC). For sites 1 - 9 and 36 - 44, mixes were based on Environment and Climate Change Canada (ECCC) water masses maps. For the remaining sites (10 - 35), mixes were provided by Jean Morin (ECCC). LSF = Lake Saint-François, LSL = Lake Saint-Louis, FC = Fluvial corridor, LSP = Lake Saint-Pierre, FE = Fluvial estuary.

Section	Site	Latitude	Longitude	May	August
				Water Mass (%)	Water Mass (%)
LSF	1	45.1115	-74.446	100 GL	100 GL
	2	45.1186	-74.4612	100 GL	100 GL
	3	45.128	-74.4784	100 GL	100 GL
	4	-	-	-	100 GL
	5	45.2273	-74.2145	100 GL	100 GL
	6	-	-	-	100 GL
LSL	7	45.3974	-73.7892	100 GL	100 GL
	8	45.4099	-73.8103	100 GL	100 GL
FC	10	45.5326	-73.5282	45 GL / 55 CRS	-
	11	45.5326	-73.5316	100 GL	84 GL / 16 CRS
	12	45.5328	-73.5371	100 GL	100 GL
	13	45.73298	-73.41667	100 GL	2 MIP / 99 GL
	14	45.7354	-73.4225	100 GL	1 MIP / 99 GL
	15	45.73628	-73.43353	50 GL / 50 OTT	-
	16	45.7402	-73.4365	48 ASS / 52 OTT	-
	17	45.9334	-73.213	100 GL	3 MIP / 98 GL
	18	45.9354	-73.2222	69 GL / 31 OTT	7 MIP / 93 GL
19	45.9375	-73.2317	3 ASS / 97 OTT	75 MIP / 26 GL	
LSP	20	46.0594	-73.077	60 GL / 40 RICH	75 GL / 25 RICH
	21	46.072	-73.0824	58 GL / 42 OTT	67 GL / 33 RICH
	23	46.1625	-72.8634	52 GL / 48 RICH	43 RICH / 57 GL
	24	46.1783	-72.8776	100 GL	26 RICH / 74 GL
	25	46.192	-72.8909	100 GL	6 MIP / 94 GL
	26	46.2012	-72.9015	51 GL / 49 OTT	39 MIP / 62 GL
	27	46.2058	-72.9076	36 GL / 64 OTT	52 MIP / 49 GL

	28	46.2139	-72.9149	96 OTT / 4 MASK	-
	29	46.2228	-72.7154	44 GL / 56 RICH	-
	30	46.2342	-72.733	100 GL	42 RICH / 58 GL
	31	46.2389	-72.7396	100 GL	30 RICH / 70 GL
	32	46.2441	-72.7472	100 GL	23 RICH / 77 GL
	33	46.2524	-72.7552	59 GL / 41 OTT	27 MIP / 74 GL
	34	46.2581	-72.7625	32 GL / 68 OTT	52 MIP / 48 GL
	35	46.265	-72.7697	85 OTT / 15 MASK	-
	36	46.3581	-72.4882	44 GL / 56 RICH	42 RICH / 58 GL
	37	46.3612	-72.4976	100 GL	27 RICH / 73 GL
	38	46.3625	-72.5002	30 GL / 65 OTT / 5 MASK	39 MIP / 61 GL
FE	39	46.6346	-71.7283	100 QC	100 QC
	40	46.6393	-71.7283	100 QC	100 QC
	41	46.6579	-71.7283	100 QC	100 QC
	42	46.7476	-71.2677	100 QC	100 QC
	43	46.7507	-71.271	100 QC	100 QC
	44	46.753	-71.2737	100 QC	100 QC

Table S2b. Site-by-edge matrix for August hydroperiod.

Sites	Edges																											
	1	2	3	4	5	6	7	8	9	10	11	12	13	14	15	16	17	18	19	20	...	58						
1	1	0	0	0	0	0	0	0	0	0	0	0	0	0	0	0	0	0	0	0	...	0						
2	0	1	0	0	0	0	0	0	0	0	0	0	0	0	0	0	0	0	0	0	...	0						
3	0	0	1	0	0	0	0	0	0	0	0	0	0	0	0	0	0	0	0	0	...	0						
4	1	0	0	1	0	0	0	0	0	0	0	0	0	0	0	0	0	0	0	0	...	0						
5	0	1	0	0	1	0	0	0	0	0	0	0	0	0	0	0	0	0	0	0	...	0						
6	0	0	1	0	0	1	0	0	0	0	0	0	0	0	0	0	0	0	0	0	...	0						
7	1	0	0	1	0	0	1	0	0	0	0	0	0	0	0	0	0	0	0	0	...	0						
8	1	1	1	1	1	1	0	1	1	1	0	0	0	0	0	0	0	0	0	0	...	0						
11	1	1	1	1	1	1	1	1	1	1	1	1	0	0	0	0	0	0	0	0	...	0						
12	1	1	1	1	1	1	0	1	1	1	0	0	1	0	0	0	0	0	0	0	...	0						
13	1	1	1	1	1	1	1	1	1	1	1	1	0	1	0	0	0	0	0	0	...	0						
14	1	1	1	1	1	1	1	1	1	1	1	1	1	0	1	1	0	0	0	0	...	0						
17	1	1	1	1	1	1	1	1	1	1	1	1	1	1	1	1	0	1	1	0	...	0						
18	1	1	1	1	1	1	1	1	1	1	1	1	1	0	1	1	0	0	0	1	...	0						
19	1	1	1	1	1	1	0	1	1	1	0	0	1	0	0	0	1	0	0	0	...	0						
20	1	1	1	1	1	1	1	1	1	1	1	1	1	1	1	0	1	1	0	...	0							
⋮	⋮	⋮	⋮	⋮	⋮	⋮	⋮	⋮	⋮	⋮	⋮	⋮	⋮	⋮	⋮	⋮	⋮	⋮	⋮	⋮	...	⋮						
44	1	1	1	1	1	1	1	1	1	1	1	1	1	0	1	1	1	0	0	1	...	1						

Table S2c. Weight vector for May hydroperiod.

Edges																											
1	2	3	4	5	6	7	8	9	10	11	12	13	14	15	16	17	18	19	20	...	68						
100	100	100	100	33.3	100	33.3	33.3	100	50	50	100	100	50	50	25	25	50	52	48	...	100						

Table S2d. Weight vector for August hydroperiod.

Edges																											
1	2	3	4	5	6	7	8	9	10	11	12	13	14	15	16	17	18	19	20	...	58						
100	100	100	100	100	100	100	33.3	33.3	33.3	50	50	100	100	50	50	26	50	50	93	...	100						

Table S3. Mean abundance ($\text{ind}\cdot\text{m}^{-3}$) \pm standard deviation (SD) of crustacean groups and species in the biogeographical zones of the St. Lawrence River. FSZ: Fluvial Section Zone, FEZ: Fluvial-Estuary Zone, ETZ: Estuarine Transition Zone.

Group	Family	Genus	Species	May			August		
				FSZ (N=33) mean \pm SD	FEZ (N=10) mean \pm SD	ETZ (N=7) mean \pm SD	FSZ (N=29) mean \pm SD	FEZ (N=10) mean \pm SD	ETZ (N=7) mean \pm SD
Cladocerans	Bosminidae	<i>Bosmina</i>	<i>coregoni</i>	4.9 \pm 11.5	4.0 \pm 7.7	0.3 \pm 0.9	3.9 \pm 7.1	0.6 \pm 1.8	
	Bosminidae	<i>Bosmina</i>	<i>sp.</i>	52.6 \pm 75.2	59.1 \pm 48.8	18.8 \pm 34.9	75.7 \pm 219	24.9 \pm 28.3	26.9 \pm 63.2
	Chydoridae	<i>Acroperus</i>	<i>sp.</i>	0.1 \pm 0.8			4.8 \pm 17.4		
	Chydoridae	<i>Alona</i>	<i>guttata</i>		0.04 \pm 0.1				
	Chydoridae	<i>Alona</i>	<i>sp.</i>	1.4 \pm 2.3	0.4 \pm 0.9		5.9 \pm 13.2	5.5 \pm 10.4	
	Chydoridae	<i>Alonella</i>	<i>sp.</i>	0.1 \pm 0.4			4.1 \pm 13.3	0.2 \pm 0.4	
	Chydoridae	<i>Camptocercus</i>	<i>sp.</i>	0.03 \pm 0.2			5.7 \pm 16.8	6.1 \pm 14.2	
	Chydoridae	<i>Chydorus</i>	<i>brevilabris</i>	0.2 \pm 1.0					
	Chydoridae	<i>Chydorus</i>	<i>sp.</i>	16.2 \pm 20.0	5.4 \pm 7.1	0.3 \pm 0.9	12.7 \pm 62.0	1.8 \pm 2.2	
	Chydoridae	<i>Eurycercus</i>	<i>sp.</i>		0.04 \pm 0.1	0.3 \pm 0.9	0.8 \pm 1.6	0.2 \pm 0.6	
	Chydoridae	<i>Leydigia</i>	<i>quadrangularis</i>	0.3 \pm 1.2	0.2 \pm 0.6				
	Chydoridae	<i>Leydigia</i>	<i>sp.</i>				1.0 \pm 3.9	0.1 \pm 0.2	
	Chydoridae	<i>Pleuroxus</i>	<i>denticulatus</i>	0.05 \pm 0.3	0.6 \pm 2.0				
	Chydoridae	<i>Pleuroxus</i>	<i>sp.</i>		0.4 \pm 1.2		2.0 \pm 9.6	0.04 \pm 0.1	
	Chydoridae	-	-	1.4 \pm 2.6			3.6 \pm 11.0	0.6 \pm 1.8	
	Daphniidae	<i>Ceriodaphnia</i>	<i>sp.</i>	0.03 \pm 0.1			11.2 \pm 17.8	3.7 \pm 7.9	
	Daphniidae	<i>Daphnia</i>	<i>ambigua</i>	0.3 \pm 0.9	0.4 \pm 1.2			0.2 \pm 0.6	
	Daphniidae	<i>Daphnia</i>	<i>catawba</i>	0.3 \pm 1.1	0.4 \pm 1.2		0.03 \pm 0.1		
	Daphniidae	<i>Daphnia</i>	<i>longiremis</i>	0.4 \pm 1.2	0.2 \pm 0.7				
	Daphniidae	<i>Daphnia</i>	<i>parvula</i>	0.1 \pm 0.3					
	Daphniidae	<i>Daphnia</i>	<i>pulex</i>	0.03 \pm 0.1					
	Daphniidae	<i>Daphnia</i>	<i>pulicaria</i>	0.4 \pm 1.1	0.04 \pm 0.1			0.3 \pm 0.7	
	Daphniidae	<i>Daphnia</i>	<i>retrocurva</i>	0.5 \pm 2.2			0.1 \pm 0.5		
	Daphniidae	<i>Daphnia</i>	<i>sp.</i>	1.8 \pm 3.8	0.8 \pm 1.8	4.1 \pm 11.0	6.4 \pm 17.2	0.2 \pm 0.5	
	Daphniidae	<i>Scapholeberis</i>	<i>kingi</i>	0.2 \pm 1.1					
	Daphniidae	<i>Scapholeberis</i>	<i>sp.</i>				0.1 \pm 0.4		
	Daphniidae	-	-				0.1 \pm 0.4		
	Holopediidae	<i>Holopedium</i>	<i>sp.</i>		0.2 \pm 0.6				
	Ilyocryptidae	<i>Ilyocryptus</i>	<i>spinifer</i>				0.1 \pm 0.4	1.2 \pm 2.2	
	Polyphemidae	<i>Polyphemus</i>	<i>sp.</i>				0.4 \pm 2.1		
	Sididae	<i>Diaphanosoma</i>	<i>brachyurum</i>	0.5 \pm 2.7					
	Sididae	<i>Diaphanosoma</i>	<i>sp.</i>	0.2 \pm 1.3			8.6 \pm 33.2	0.7 \pm 1.5	
Sididae	<i>Sida</i>	<i>sp.</i>				2.4 \pm 4.9	3.0 \pm 2.9		
Total	7	17	at least* 23	81.9 \pm 94.6	72.2 \pm 52.4	23.9 \pm 33.9	149 \pm 321	49.1 \pm 50.4	31.6 \pm 68.7

Calanoids		Copepodites		7.8 ± 9.0	16.9 ± 13.2	449 ± 682	84.2 ± 209	172 ± 151	1249 ± 1872
	Acartiidae	<i>Acartia</i>	<i>longiremis</i>			344 ± 900			23.4 ± 29.9
	Diaptomidae	<i>Leptodiaptomus</i>	<i>minutus</i>	0.2 ± 0.9					
	Diaptomidae	<i>Leptodiaptomus</i>	<i>sicilis</i>	0.2 ± 0.9	0.4 ± 0.8		0.1 ± 0.4		
	Diaptomidae	<i>Skistodiaptomus</i>	<i>oregonensis</i>	0.1 ± 0.6			0.7 ± 1.3	0.5 ± 1.5	
	Diaptomidae	<i>Skistodiaptomus</i>	<i>reighardi</i>	0.05 ± 0.3			0.4 ± 1.0		
	Temoridae	<i>Epischura</i>	<i>lacustris</i>	0.4 ± 1.2					
	Temoridae	<i>Eurytemora</i>	<i>affinis</i>	0.003 ± 0.02		153 ± 181	4.0 ± 7.3	16.2 ± 15.8	709 ± 1601
	Temoridae	<i>Eurytemora</i>	<i>herdmani</i>			0.7 ± 1.8			1.5 ± 4.1
Total	3	5	8	8.7 ± 9.3	17.3 ± 12.9	947 ± 1507	89.4 ± 210	188 ± 159	1990 ± 3408
Cyclopoids		Copepodites		230 ± 239	315 ± 211	141 ± 137	33.7 ± 39.5	10.9 ± 5.3	0.8 ± 1.7
	Cyclopidae	<i>Acanthocyclops</i>	<i>carolinianus</i>	0.2 ± 1.2					
	Cyclopidae	<i>Acanthocyclops</i>	<i>robustus</i>	0.2 ± 0.6	0.4 ± 1.0		1.2 ± 4.2	1.2 ± 2.5	
	Cyclopidae	<i>Acanthocyclops</i>	<i>venustoides</i>	0.5 ± 1.8	0.04 ± 0.1		0.02 ± 0.1		
	Cyclopidae	<i>Diacyclops</i>	<i>nanus</i>	0.04 ± 0.2					
	Cyclopidae	<i>Diacyclops</i>	<i>thomasi</i>	12.1 ± 13.5	14.4 ± 13.2	10.1 ± 11.2	0.1 ± 0.3		
	Cyclopidae	<i>Eucyclops</i>	<i>elegans</i>	0.3 ± 1.6			0.2 ± 1.0	0.3 ± 0.6	
	Cyclopidae	<i>Eucyclops</i>	<i>pectinifer</i>	1.3 ± 2.6	0.04 ± 0.1		29.6 ± 144	2.3 ± 4.9	
	Cyclopidae	<i>Eucyclops</i>	<i>prionophorus</i>	0.5 ± 1.2	0.2 ± 0.5		1.2 ± 2.4	0.04 ± 0.1	
	Cyclopidae	<i>Halicyclops</i>	<i>fosteri</i>					29.8 ± 94.2	507 ± 780
	Cyclopidae	<i>Macrocyclus</i>	<i>albidus</i>				0.05 ± 0.2	0.2 ± 0.6	
	Cyclopidae	<i>Mesocyclops</i>	<i>americanus</i>	0.04 ± 0.2			0.4 ± 1.7	0.4 ± 0.8	
	Cyclopidae	<i>Mesocyclops</i>	<i>edax</i>	0.2 ± 0.9	0.04 ± 0.1		3.4 ± 16.9		
	Cyclopidae	<i>Microcyclops</i>	<i>rubellus</i>	0.5 ± 1.6	0.6 ± 1.2		1.7 ± 6.1	0.3 ± 0.7	
	Cyclopidae	<i>Orthocyclops</i>	<i>modestus</i>	0.04 ± 0.2					
	Cyclopidae	<i>Paracyclops</i>	<i>chiltoni</i>	0.1 ± 0.4			1.1 ± 4.4	0.2 ± 0.6	
	Cyclopidae	<i>Paracyclops</i>	<i>poppei</i>	0.04 ± 0.2					
	Cyclopidae	<i>Tropocyclops</i>	<i>prasinus</i>	2.3 ± 6.0	2.9 ± 3.7		2.5 ± 5.6	0.4 ± 0.7	
Total	1	10	17	248 ± 253	333 ± 222	151 ± 136	73.9 ± 156	46.0 ± 89.6	514 ± 781
Harpacticoids		Copepodites		1.0 ± 2.7	0.1 ± 0.2	107 ± 169	0.7 ± 1.3		
	Ameiridae	<i>Nitokra</i>	<i>hibernica</i>	1.5 ± 3.6	1.7 ± 2.8		3.4 ± 4.1	1.3 ± 1.9	0.1 ± 0.3
	Ameiridae	<i>Nitokra</i>	sp.	0.2 ± 1.0			0.1 ± 0.4		
	Canthocamptidae	<i>Attheyella</i>	<i>americana</i>	0.1 ± 0.7			0.005 ± 0.03		
	Canthocamptidae	<i>Bryocamptus</i>	<i>hiemalis</i>	0.05 ± 0.3					
	Canthocamptidae	<i>Bryocamptus</i>	<i>hutchinsoni</i>				0.03 ± 0.1		
	Canthocamptidae	<i>Bryocamptus</i>	<i>minutus</i>	0.3 ± 1.7					
	Canthocamptidae	<i>Bryocamptus</i>	<i>nivalis</i>		0.7 ± 1.9				
	Canthocamptidae	<i>Bryocamptus</i>	<i>zschokkei</i>	0.2 ± 0.7					
	Canthocamptidae	<i>Canthocamptus</i>	<i>robertcokeri</i>	0.3 ± 1.7					
	Canthocamptidae	<i>Canthocamptus</i>	sp.				0.03 ± 0.2		

Canthocamptidae	<i>Canthocamptus</i>	<i>staphylinoides</i>	1.5 ± 4.1						
Canthocamptidae	<i>Canthocamptus</i>	<i>vagus</i>	0.2 ± 0.7						
Canthocamptidae	<i>Elaphoidella</i>	<i>bidens</i>	0.1 ± 0.4	0.3 ± 1.0	0.4 ± 1.1	0.2 ± 0.5	0.1 ± 0.2		
Canthocamptidae	<i>Heteropsyllus</i>	<i>nunni</i>	0.1 ± 0.8			0.2 ± 0.8	0.1 ± 0.2		
Canthocamptidae	<i>Mesochra</i>	<i>alaskana</i>	0.7 ± 2.4	0.3 ± 0.9		0.5 ± 2.3	2.5 ± 6.7		
Diosaccidae	<i>Schizopera</i>	<i>borutzkyi</i>	0.1 ± 0.4	2.7 ± 3.2	5.6 ± 13.7	1.1 ± 1.6	1.3 ± 2.9		
Ectinosomatidae	<i>Halectinosoma</i>	<i>curticorne</i>		0.2 ± 0.7	343 ± 479			391 ± 847	
Ectinosomatidae	<i>Microstella</i>	<i>norvegica</i>			2.6 ± 6.9				
Laophontidae	<i>Onychocamptus</i>	<i>mohammed</i>	0.6 ± 1.6	0.4 ± 1.4	0.4 ± 1.1	9.9 ± 39.9	2.4 ± 3.4		
Tachidiidae	<i>Microarthridion</i>	<i>falax</i>			0.2 ± 0.5				
Tachidiidae	<i>Microarthridion</i>	<i>littorale</i>			2.1 ± 3.9			14.1 ± 30.2	
Total	6	12	at least 19	6.9 ± 8.0	6.6 ± 4.8	462 ± 641	16.1 ± 39.2	7.6 ± 11.0	410 ± 889
Total	17	44	at least 67	346	429	1584	329	291	2946

*at least: Taxa which were not identified to species level were not counted in the total number of species when at least one other known species of the same genus was present.

Table S4. R^2_a statistics from the global RDA analyses of the AEM models after different species data transformations. Bold values: highest R^2_a values per hydroperiod. Boxed value for each hydroperiod: AEM model–weighting–transformation combination with highest R^2_a retained for the forward selection of the AEM eigenfunctions.

		Transformations				
AEM Model	Weights on the edges	Hellinger	Log-chord	Chord	Chi-square	
May	Mixing with tributaries	yes	0.197	0.341	-0.181	0.237
		no	0.328	0.407	0.041	0.390
	Mixing without tributaries	yes	0.228	0.360	-0.140	0.149
		no	0.356	0.472	0.018	0.402
	No mixing with tributaries	yes	0.177	0.245	-0.050	0.191
		no	0.297	0.375	0.017	0.404
August	No mixing without tributaries	yes	0.121	0.201	-0.126	0.104
		no	0.275	0.326	-0.008	0.362
	Mixing with tributaries	yes	0.552	0.535	0.522	0.447
		no	0.610	0.583	0.593	0.484
	Mixing without tributaries	yes	0.516	0.485	0.451	0.362
		no	0.574	0.566	0.551	0.450
	No mixing with tributaries	yes	0.544	0.522	0.517	0.437
		no	0.600	0.564	0.571	0.463
	No mixing without tributaries	yes	0.518	0.497	0.466	0.353
		no	0.534	0.540	0.504	0.391

Figure S1. Bubble plot maps presenting the fitted values of zooplankton on the significant canonical axes of the best RDA model with the selected AEMs in (a) May and (b) August. In May, (c) calanoids, (d) cladocerans, (e) cyclopoids, and (f) harpacticoids are bubble plots of zooplankton log-chord-transformed abundances. In August, (g) calanoids, (h) cladocerans, (i) cyclopoids, and (j) harpacticoids are bubble plots of zooplankton Hellinger-transformed abundances. Bubble size is proportional to the value associated to it. Black reflects positive values, while white corresponds to negative values. Signs are arbitrary in AEM eigenfunctions.

